MOLECULAR AND CELLULAR BIOLOGY, Nov. 2004, p. 10000–10015 Vol. 24, No. 22
0270-7306/04/$08.00+0 DOI: 10.1128/MCB.24.22.10000–10015.2004

Extracellular Signal-Regulated Kinase 1c (ERK1c), a Novel 42-Kilodalton ERK, Demonstrates Unique Modes of Regulation, Localization, and Function†

Daniel M. Aebersold,‡ Yoav D. Shaul,‡ Yuval Yung,‡ Nirit Yarom, Zhong Yao, Tamar Hanoch, and Rony Seger*

Department of Biological Regulation, Weizmann Institute of Science, Rehovot, Israel

Received 19 March 2004/Returned for modification 13 April 2004/Accepted 27 August 2004

Extracellular signal-regulated kinases (ERKs) are signaling molecules that regulate many cellular processes. We have previously identified an alternatively spliced 46-kDa form of ERK1 that is expressed in rats and mice and named ERK1b. Here we report that the same splicing event in humans and monkeys causes, due to sequence differences in the inserted introns, the production of an ERK isoform that migrates together with the 42-kDa ERK2. Because of the differences of this isoform from ERK1b, we named it ERK1c. We found that its expression levels are about 10% of ERK1. ERK1c seems to be expressed in a wide variety of tissues and cells. Its activation by MEKs and inactivation by phosphatases are slower than those of ERK1, which is probably the reason for its differential regulation in response to extracellular stimuli. Unlike ERK1, ERK1c undergoes monoubiquitination, which is increased with elevated cell density concomitantly with accumulation of ERK1c in the Golgi apparatus. Elevated cell density also causes enhanced Golgi fragmentation, which is facilitated by overexpression of native ERK1c and is prevented by dominant-negative ERK1c, indicating that ERK1c mediates cell density-induced Golgi fragmentation. The differential regulation of ERK1c extends the signaling specificity of MEKs after stimulation by various extracellular stimuli.

Extracellular signal-regulated kinases (ERKs) 1 and 2 (ERK1 and ERK2, which are 44 and 42 kDa, respectively) are key signaling enzymes that are activated by a large number of extracellular stimuli and play an important role in physiological processes, such as proliferation, differentiation, and development (28, 32, 40). ERKs are ubiquitously expressed and share a high degree of similarity (85% [5]). Under most conditions, ERK1 and ERK2 demonstrate identical patterns of regulation, which is mainly manifested in their activation by MEK1 and MEK2 (MEKs) through the phosphorylation of threonine and tyrosine in their characteristic Thr-Glu-Tyr motif. These two isoforms also share substrate recognition and subcellular localization, suggesting a redundant functionality of these ERKs (34). Consistent with these observations, ERK1 knockout mice are viable, without any apparent defects, which might be due to increased levels of ERK2 expression that compensate for the lack of ERK1 (24). On the other hand, ERK2 knockout mice die as embryos, due to failure in mesoderm induction, which is not compensated for by ERK1 that is not expressed at this stage of embryonic development (45). The ability of the ERKs to transmit different and even opposing signals despite the pronounced similarities between the two ERK isoforms raises the question of how is the specificity of the different signals regulated.

It has previously been demonstrated that signaling specificity is determined by duration and strength of the signals (23) as well as compartmentalization (29, 39). Another mechanism that contributes to specificity is the extensive cross talk and interplay between the ERK cascade and other intracellular signaling pathways, including the other kinase cascades (e.g., c-Jun N-terminal kinase (JNK), p38 mitogen-activated protein kinase (MAPK), and protein kinase B [30]). However, these mechanisms do not fully explain the large diversity of different targets that are activated by the ERKs in response to different stimuli. An important factor that contributes to specificity within other cascades is the existence of several similar isoforms at each level of the cascade. An example of such diversity is the 10 isoforms of JNK that result from alternative splicing of three JNK genes (15). A comparison of the binding activity of the JNK isoforms demonstrated that the JNK proteins differ in their interaction with ATF2, Elk1, and the Jun transcription factors. Individual members of the JNK group may therefore selectively target specific transcription factors (15). Other MAPK components are also present as multiple alternatively spliced isoforms (44), including MKK7 (41), MKK6 (17), MEK5 (11), and ERK5 (44).

A multiplicity of components may participate in the diversification of signals that are transmitted through the ERK cascade as well. Indeed, differences in the regulation and protein interaction of ERK1 and ERK2 have been demonstrated in several systems. Thus, it was shown that ERK1, but not ERK2, can interact with MP1 (33) or Syk (43), and ERK2 may play a specific role in embryogenesis (9). In addition, alternatively spliced isoforms of MEK1 and ERKs are known to exist and may lead to differential regulation of signaling. An alternatively spliced form of MEK1, named MEK1b (35), was reported to lack kinase activity (49) and may inhibit signaling in specific cellular compartments. In addition, an alternatively spliced form of ERK2 was identified at the mRNA level, but it

* Corresponding author. Mailing address: Department of Biological Regulation, Weizmann Institute of Science, Rehovot 76100, Israel. Phone: 972-8-9343602. Fax: 972-8-9344116. E-mail: rony.seger@weizmann.ac.il.

‡ D.M.A., Y.D.S., and Y.Y. contributed equally to the manuscript.

† Supplemental material for this article may be found at http://mcb.asm.org/.

is not clear whether it is expressed as a protein in any tissue or organism (14).

Another alternatively spliced form of ERKs is the ERK1b that we identified as an alternatively spliced form of ERK1 that is expressed in rats and mice as a 46-kDa protein and which is probably the same protein as the poorly characterized ERK4 (4, 7, 25). We have shown that this 46-kDa ERK isoform contains a 26-amino-acid insertion between residues 340 and 341 of ERK1 (48). Although under most conditions ERK1b is regulated similarly to ERK1 and ERK2, we found conditions under which the activation of ERK1b by extracellular stimuli differs from that of the other ERKs. Biochemical studies demonstrated that the differences of regulation are due to the site of insertion that interferes with the integrity of the cytosolic retention sequence (CRS)/common docking (CD) motif of ERK1 (31, 38) and not due to the sequence of the insert itself. This insertion results in an altered interaction with MEK1, which leads to a different subcellular localization of ERK1b. This kinase exhibits decreased ability to phosphorylate its substrate, transcription factor Elk1, and importantly, the ability of ERK1b to interact with phosphatases PTP-SL and MKP3 is defective, which dramatically affects its down-regulation process (47).

One important observation in our previous studies was that ERK1b mRNA might exist not only in rats but also in humans. However, we were unable to identify a 46-kDa ERK in humans under any condition used (48). Therefore, we undertook to identify the putative human ERK1b protein and study its regulation. We found that the same alternative splicing event that forms the rat ERK1b by including intron 7 in the mRNA of ERK1 also occurs in humans. However, unlike the 78 bp inserted in rat ERK1 mRNA, the human insert consists of 103 bp. Although this insertion is ~35% identical to the rat sequence, the human insert contains a stop codon; therefore, the human protein is shorter than ERK1 and migrates together with ERK2 as a 42-kDa protein on sodium dodecyl sulfate (SDS)-polyacrylamide gels. Because of its different properties, we named this protein ERK1c and found that it is also expressed in monkeys. ERK1c is an active protein kinase that can undergo monoubiquitination, but not polyubiquitination, especially in confluent cells. This modification seems to direct ERK1c to the Golgi apparatus where it induces Golgi fragmentation. The expression of this differentially regulated ERK1c may broaden the specificity of the ERK cascade and allow it to regulate distinct and even opposing cellular functions under various conditions.

MATERIALS AND METHODS

Materials. Epidermal growth factor (EGF), 4β-phorbol 12-myristate 13-acetate (TPA), protein A- or protein G-Sepharose, and myelin basic protein (MBP) were obtained from Sigma (St. Louis, Mo.). Antibodies (Abs) against doubly phosphorylated ERK (pERK), general ERK (gERK), hemagglutinin tag (HA), Golgi apparatus marker p58, and ubiquitin were from Sigma Israel. Anti-ERK2 Ab (C14), anti-Elk1 Ab (l-20), anti-pElk1 Ab (antibody against phosphorylated Elk1), and anti-HA Ab were from Santa Cruz Biotechnology (Santa Cruz, Calif.), and anti-green fluorescent protein (GFP) Ab was from Roche Diagnostics (Indianapolis, Ind.). Alkaline phosphatase-conjugated secondary Ab and the developing substrate nitroblue tetrazolium or 5-bromo-4-chloro-3-indolylphosphate were purchased from Promega (Madison, Wis.). Rhodamine-conjugated secondary Ab was from Jackson Immunoresearch (West Grove, Pa.). To-Pro-3 was from Molecular Probes (Eugene, Oreg.). Elk1 fusion protein was from Cell Signaling (Beverly, Mass.).

Buffers. Buffer A consisted of 50 mM β-glycerophosphate (pH 7.3), 1.5 mM EGTA, 1 mM EDTA, 1 mM dithiothreitol (DTT), and 0.1 mM sodium vanadate. Buffer H consisted of 50 mM glycerophosphate (pH 7.3), 1.5 mM EGTA, 1 mM EDTA, 1 mM DTT, 0.1 mM sodium vanadate, 1 mM benzamidine, 10 μg of aprotinin per ml, 10 μg of leupeptin per ml, and 2 μg of pepstatin A per ml. Buffer RM (3× reaction mixture) consisted of 30 mM $MgCl_2$, 1.5 mM DTT, 75 mM β-glycerophosphate (pH 7.3), 0.15 mM sodium vanadate, 3.75 mM EGTA, 30 μM calmidazolium, and 2.5 mg of bovine serum albumin per ml. Radioimmunoprecipitation assay (RIPA) buffer consisted of 137 mM NaCl, 20 mM Tris (pH 7.4), 10% (vol/vol) glycerol, 1% Triton X-100, 0.5% (wt/vol) deoxycholate, 0.1% (wt/vol) SDS, 2 mM EDTA, 1 mM phenylmethylsulfonyl fluoride, and 20 μM leupeptin. Buffer LS (low-stringency buffer) consisted of 20 mM HEPES (pH 8.0), 2 mM $MgCl_2$, and 2 mM EGTA.

RT-PCR and constructs. Total RNA was prepared using TRI reagent (Molecular Research Center, Inc.) according to the manufacturer's instructions. To remove traces of genomic DNA, RNA preparations were treated with DNase (Ambion) according to the manufacturer's instructions. Reverse transcription-PCR (RT-PCR) was performed with the Titan one-tube RT-PCR kit (Roche) following the manufacturer's protocol. The following oligonucleotides were used for cloning: ERK1-Exon1-S (GCTACACGCAGTTGCAGTACA), ERK1-Exon7-S (CTGGACCGGATGTTAACCTTTA), ERK1-Exon8-AS (GTGCTGT CTCCTGGAAGATGAG), and ERK1c-insert-AS (GGGGTGGTAGAGACA GCAAG). The full-length ERK1c was ligated into the NotI sites of pCDNA1 (Invitrogen), into the NheI and NotI sites of HA-pCDNA3 (Invitrogen), or into the ScaII sites of pEGFP-C1 (Clontech, Palo Alto, Calif.). The inactive K72A-ERK1c (KA-ERK1c) was prepared by PCR in the same vectors as the wild-type ERK1c.

Real-time PCR. Total RNA was reverse transcribed using the first-strand cDNA synthesis kit for RT-PCR (Roche) with random hexamers as primers according to the manufacturer's recommendations. Real-time PCR was performed in a LightCycler (Roche) with the FastStart DNA Master Hybridization Probes kit (Roche) following the manufacturer's instructions for the composition of the reaction mixture. The forward primers used for isoform-specific amplification are CGACGGATGAGCCAGTG for ERK1 and TGCTGTCTCTACCA CCCCA for ERK1c. The ERK1-Exon8-AS oligonucleotide was the reverse primer. The fluorescent hybridization probes for sequence-specific detection (Tib Molbiol, Berlin, Germany) were the sequences LCRed640-TGGCGAAGGTG AAGGGCTCCTC and CGCTCCTTAGGTAGGTCATCCAGCTCC-Flu. Real-time PCR was performed by a touchdown procedure (stepwise decrease of the annealing temperature for the amplification primers) using the following reaction parameters: (i) 1 cycle of 10 min at 95°C and (ii) 40 cycles, with 1 cycle consisting of 15 s at 95°C, 2 s at 64°C, a decrease from 64°C to 58°C within 5 s, and 17 s at 72°C. To generate standard curves, template dilution series (cDNA mixture in four subsequent 1:50 dilution steps) were added to the reaction mixture. Results were processed using the LightCycler software package (version 3.5.28).

Northern blot analysis. Northern blot analysis was performed on MTN (multiple tissue Northern) blots (Human 12-Lane [catalog no. 7780-1) and (human cancer cell line [catalog no. 7757-1]; Clontech) and REAL Tumor Panel IV blot (catalog no. D3804-50; ResGen). The probes used for detection were generated using the Strip-EZ PCR kit (Ambion) and labeled with [α-^{32}P]dATP according to the manufacturer's instructions, which were also followed for stripping and reprobing of the blots. PCR was done with *Taq* polymerase (Sigma). The following primers were used to generate the probes: ERK1c-insert-S (CAGTCCCCAGC AGCAGTG) and ERK1c-insert-AS for ERK1c; ERK1-Exon1-S and ERK1-Exon5-AS (CACAGACCAGATGTCGATGG) for ERK1; ERK2-Exon1-S (CA CCAACCTCTCGTACATCG) and ERK2-Exon4-AS (AGGCAAGTCATC CAATTCCA) for ERK2; and Actin-S GGCATCCTCACCCTGAAGTA and Actin-AS GGGGTGTTGAAGGTCTCAAA for β-actin. Blots were hybridized in ULTRAhyb buffer (catalog no. 8670; Ambion) following the manufacturer's protocol.

Cell culture and transfection. COS7, HeLa, and HEK-293 cells were grown in Dulbecco's modified Eagle's medium (DMEM) with 10% fetal calf serum (FCS). COS7 cells, grown in 10-cm-diameter plates, were transfected using the DEAE-dextran method using 5 μg of the desired DNA. HeLa and HEK-293 cells were transfected with polyethylenimine (PEI) (6). Briefly, the cells were grown to 50 to 70% confluence in 12-well or 6-cm-diameter plates. The plasmids (1.5 or 5 μg) were suspended in 50 or 150 μl of NaCl (150 mM) and mixed with PEI solution (50 μl or 150 μl of 3 mM PEI in 150 mM NaCl). The mixture was left at room temperature for 15 min and then incubated with the cells for 90 min. The cells were then washed and placed in DMEM containing 10% FCS. The constructs described above, as well as HA-ubiquitin (a gift from Y. Yarden, Weizmann Institute of Science), were used for these experiments.

Preparation of cell extracts. Cells were grown to subconfluence and serum starved (16 h in 0.1% FCS). After stimulation, the cells were rinsed twice with ice-cold phosphate-buffered saline (PBS) and once with ice-cold buffer A. Cells were scraped into buffer H (0.5 ml/plate) and disrupted by sonication (two 7-s pulses of 50 W). The extracts were centrifuged (20,000 × *g*, 15 min, 4°C), and the supernatants containing cytosolic and nuclear proteins were kept at 4°C. The supernatants were subjected to immunoblotting (Western blotting) as described previously (41).

Immunoprecipitation. One day after transfection, cells were serum starved (0.1% FCS) for an additional 16 h. The cells were then stimulated with either peroxovanadate (18 min) or EGF (50 ng/ml for various times) or treated with PBS for a control. After stimulation, the cells were washed, lysed, and centrifuged as described above. For the detection of endogenous ERK1c, cells were harvested with buffer H plus 1% Triton X-100. Both types of extracts were incubated (2 h, 4°C) with the indicated Abs. For determination of ERK activity and for PTP-SL coimmunoprecipitation, the beads were washed once with RIPA buffer, twice with 0.5 M LiCl, and twice with buffer A as described previously (48). The immunoprecipitates were subjected either to immunoblotting as described above or to an in vitro kinase assay.

In vitro kinase assay. The immunoprecipitated ERK proteins attached to beads were mixed with either MBP (0.5 μg per reaction mixture) or Elk1 fusion protein (0.5 μg per reaction mixture) and buffer RM that contained 100 μM [γ-^{32}P]ATP at 30°C while shaking. After 20 min, the reaction was terminated by adding 10 μl of 4× sample buffer, resolved by SDS-polyacrylamide gel electrophoresis, and subjected to autoradiography and immunoblot analysis as indicated.

Elk1 reporter assay. Elk1 activity was determined with PathDetect Elk1 *trans*-Reporting System (Stratagene, La Jolla, Calif.). Briefly, HEK-293 cells were cotransfected with the examined protein or empty vector, together with pFR-Luc containing five GAL4 response elements and a minimal promoter driving a luciferase gene, plasmid containing Elk1 fused to the DNA-binding region of GAL4, and plasmid containing *Renilla*. The luciferase and *Renilla* luminescence was measured using Dual Luciferase Reporter Assay system (Promega) reagents, according to the manufacturer's instructions. The results were calculated as a ratio of the luminescence of luciferase to that of *Renilla*.

Immunofluorescence microscopy. Cells were fixed (30 min in 3% [wt/vol] paraformaldehyde in PBS or 10 min with ice-cold methanol), followed by 5-min permeabilization in 0.2% (vol/vol) Triton X-100 in PBS (23°C). Abs were added for 1 h (23°C). After washing, coverslips were incubated with fluorescence-tagged secondary Abs for 1 h. Nuclei were visualized by 15-min incubation with 0.1 mg of 4′,6-diamidino-2-phenylindole (DAPI) per ml or To-Pro-3 in PBS. Slides were visualized using a fluorescence or confocal microscope (Bio-Rad) at a magnification of ×400.

RESULTS

Cloning of human and monkey ERK1c. The cloning and characterization of rat ERK1b, which was found to be an alternatively spliced form of ERK1 with a unique mode of regulation, prompted us to test for the existence of an ERK1b homologue in other organisms, most importantly in humans. As mentioned above, rat ERK1b contains an insert between exon 7 and exon 8 of ERK1 (intron 7); therefore, we synthesized a pair of oligonucleotide primers driven from exon 7 and exon 8 of human ERK1 (chromosome 16) in order to clone a putative insert.

RNA from several cultures of human cell lines, including HeLa, MCF-7, and DU145 cells, was extracted and treated with DNase to exclude traces of genomic DNA. RT-PCR revealed, in addition to the expected ERK1 band (~200 bp), a faint band of ~300 bp in all cell lines tested (Fig. 1A and data not shown). The 200-bp band was sequenced and found to be ERK1. Sequencing the 300-bp band revealed a 103-bp insert between exon 7 and exon 8 (Fig. 1B), which corresponded to the full length of intron 7 of this gene. Although the human insert is longer than the rat insert (78 bp [48]), it contains a stop codon at positions 55 to 57 of the insert, which results in a putative substitution of the last 40 amino acids of ERK1 with 18 amino acids of the insert (Fig. 1C).

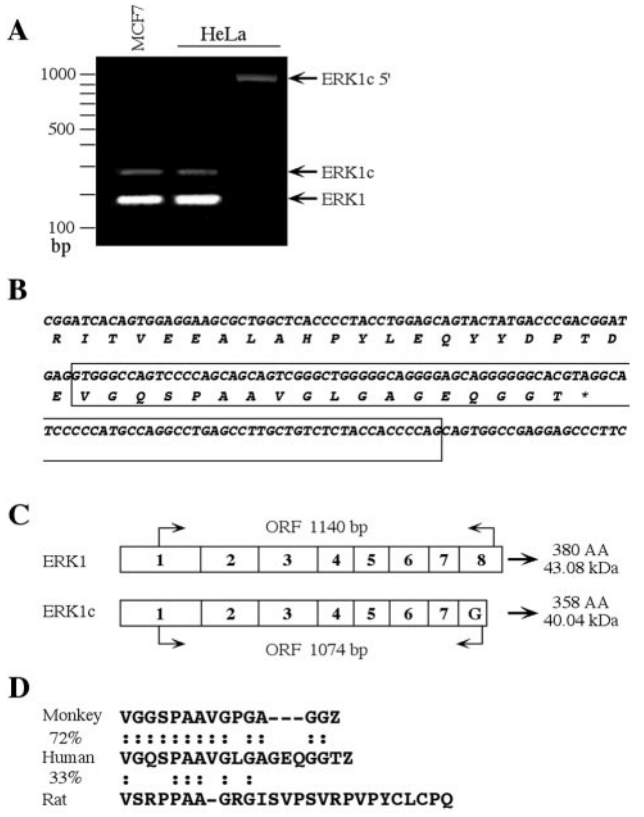

FIG. 1. Cloning of the human ERK1c. (A) RT-PCR cloning of ERK1c. The MCF7 lane shows RT-PCR with oligonucleotide primers ERK1-Exon7-S and ERK1-Exon8-AS and total RNA from MCF-7 cells as a template. The left HeLa lane shows the same RT-PCR mixture as in the MCF7 lane, except the RNA was from HeLa cells. The right HeLa lane shows RT-PCR with oligonucleotide primers ERK1-Exon1-S and ERK1c-insert-AS and total RNA from HeLa cells. The positions of the relevant fragments and DNA markers (in base pairs) are indicated at the sides of the gel. (B) cDNA and amino acid sequences of the C-terminal region of ERK1c. The unique ERK1c insert is boxed. (C) Exon organization of ERK1c and ERK1. The length of the open reading frames (ORFs), the number of amino acids (AA), and the predicted molecular mass are indicated. (D) Sequence alignment of human ERK1c, monkey ERK1c, and rat ERK1b proteins. Amino acids that are identical in the different proteins (:) and the percentage identity between the proteins are indicated. Gaps introduced to maximize alignment are indicated by the dashes.

To determine the full-length sequence and to verify the existence of the splice variant, we synthesized a pair of oligonucleotides driven from exon 1 of ERK1 and from the insert and repeated the RT-PCR. A single band (Fig. 1A) with the expected 997-bp length was sequenced and found to match the human ERK1 sequence except for the difference in the C terminus, verifying the identity of the alternatively spliced form mRNA. The predicted molecular mass of the alternatively spliced form is 40 kDa (Fig. 1B and C), which is close to that of ERK2 (41 kDa).

To clone a putative monkey ERK1c, the same approach was repeated with monkey RNA (COS7 cells), which again revealed a weak band containing an insert in a position similar to

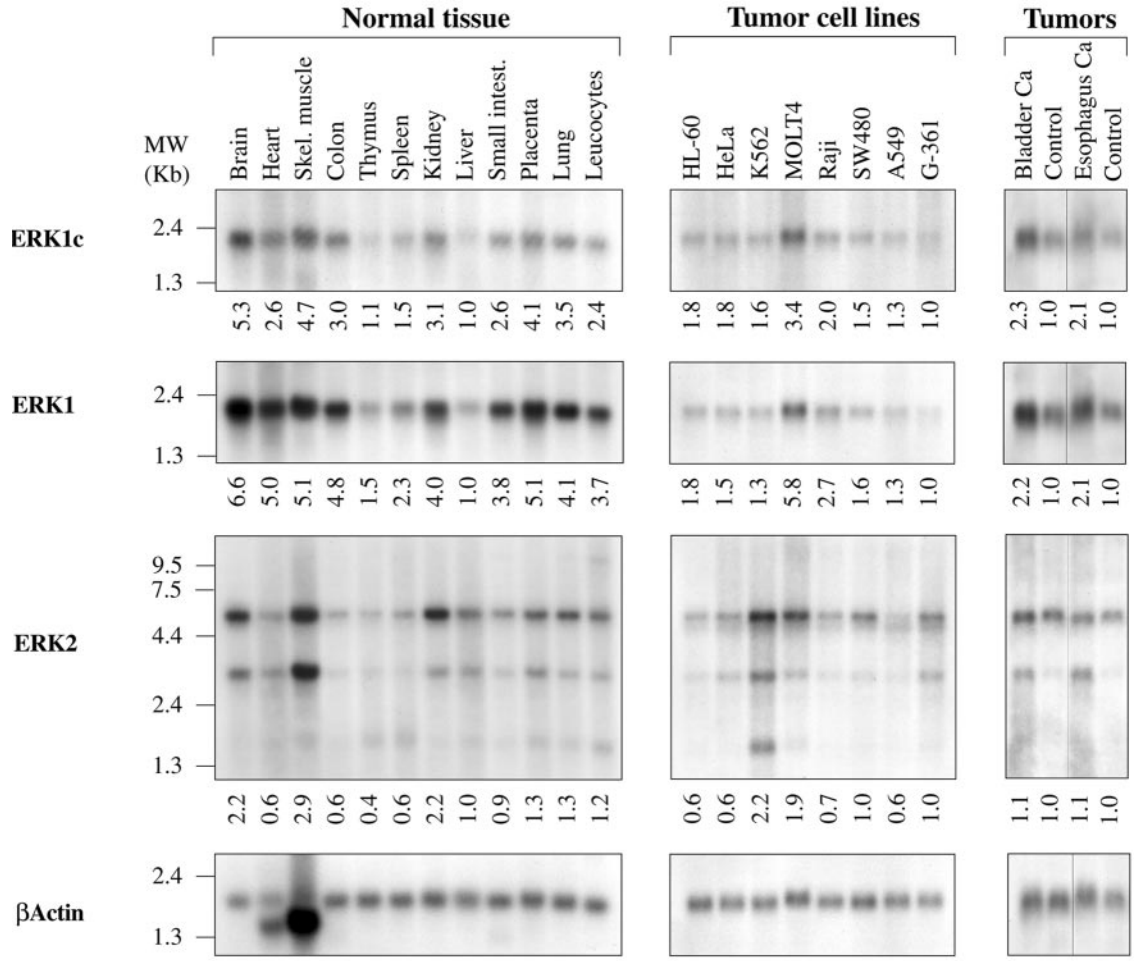

FIG. 2. Distribution of ERK1c mRNA in cells and tissues. Northern blot analysis was performed on human tissues (MTN blots; Clontech), human cancer cell lines (MTN blots; Clontech), and human tumor blots (ResGen). The specific tissue, cell line, or tumor is indicated (Skel. muscle, skeletal muscle; Small intest., small intestine; Bladder Ca, bladder cancer). The probes used for detection were generated as described in Materials and Methods. The following probes were used: ERK1c unique sequence (ERK1c), human ERK1 N terminus (ERK1), human ERK2 N terminus (ERK2), and actin. Blots were hybridized in ULTRAhyb hybridization buffer (catalog no. 8670; Ambion) following the manufacturer's protocol. The positions of the RNA markers are indicated to the left of the gels. Relative expression was calculated by using a densitometer (model 690; Bio-Rad) and is indicated under the gels.

that in human RNA. The monkey insert was found to contain a stop codon that results in substitution of the C-terminal residues by 14 amino acids, and the expected molecular mass of the protein is 39.6 kDa. Alignment of the insert sequences of human ERK1c, monkey ERK1c, and rat ERK1b (Fig. 1D) shows considerable conservation between the human and monkey sequences (72%) and less conservation between the human and rat sequences (33%). Screening the National Center for Biotechnology Information (NCBI) data bank for homologous sequences to the unique 18-amino-acid sequence of ERK1c revealed no significant similarity to any known protein. Thus, the data indicate that similar splicing processes that give rise to the 46-kDa ERK1b in rats and mice result in a shorter, ~40-kDa protein in humans and monkeys. We called the human and monkey isoform ERK1c to distinguish it from ERK1b, which although it is formed by a similar splicing process, has different molecular characteristics.

Tissue distribution and quantitative expression of ERK1c. We then examined the amount and distribution of human ERK1c in various cell types and tissues. Northern blot analysis revealed that the mRNA of ERK1c is ubiquitously expressed, though at different levels, in all tissues examined (Fig. 2). In normal tissue, the highest expression levels were found in brain and placenta, whereas the liver, thymus, and spleen featured the lowest mRNA levels. This pattern of distribution was somewhat different from that observed when the blots were exposed to a probe recognizing ERK1. However, it should be noted that the prepared ERK1 probe also recognized ERK1c (but the ERK1c probe did not recognize ERK1), which means that the actual relative differences in expression between the two mRNAs in different tissues may be even bigger than the differences seen in this blot (Fig. 2). Therefore, these results suggest that ERK1c mRNA is ubiquitous and that its expression may be regulated at the level of gene expression and at the level of the alternative splicing machinery. On the other hand, the relative mRNA levels of ERK2, which is normally ex-

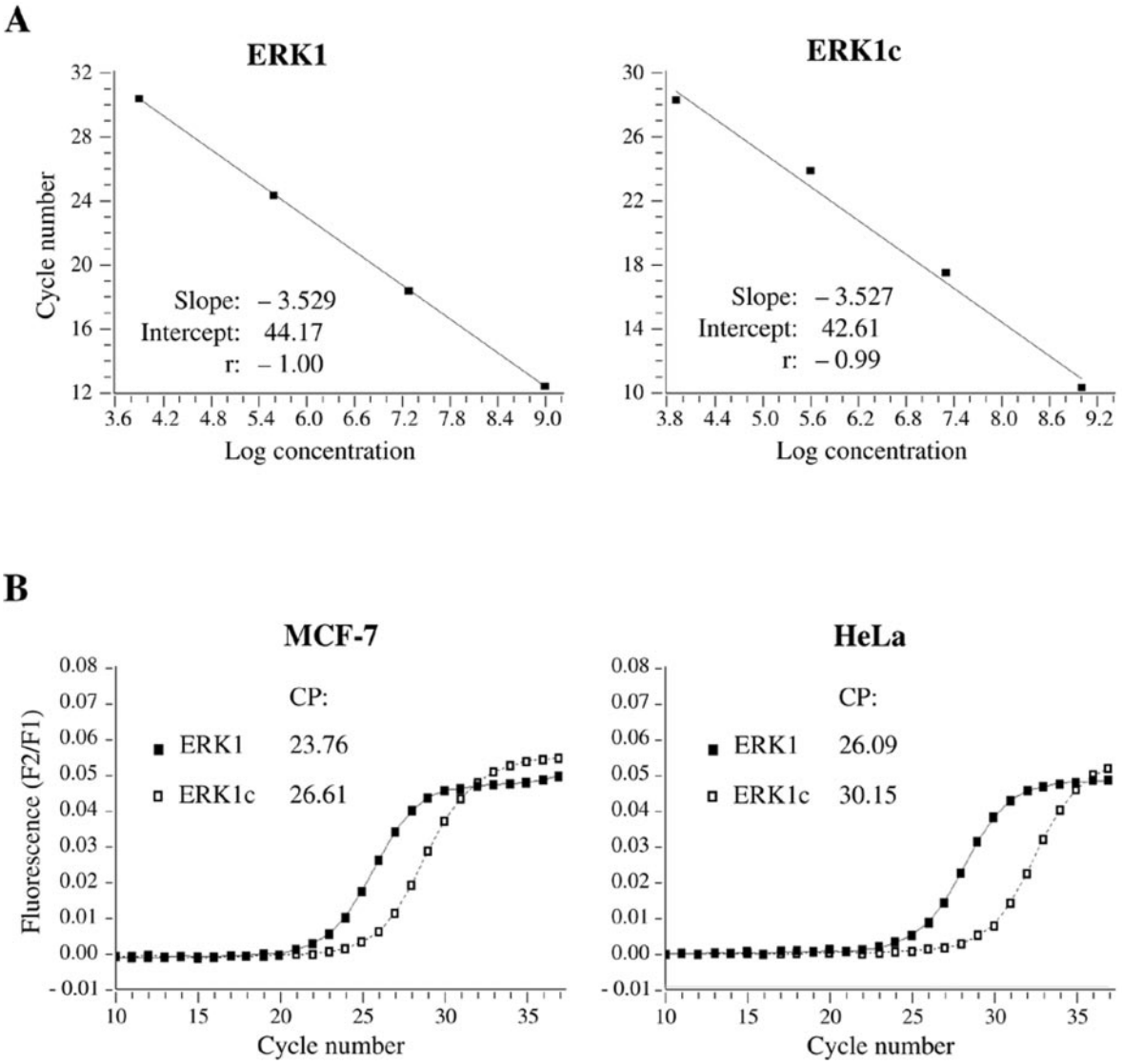

FIG. 3. Relative expression of ERK1c and ERK1 in MCF7 and HeLa cells. (A) Real-time PCR was performed in a LightCycler (Roche) with the FastStart DNA Master Hybridization Probes kit (Roche), following the manufacturer's instructions for the composition of the reaction mixture. The fluorescent hybridization probes for sequence-specific detection (synthesized by Tib Molbiol) were used. Real-time PCR was performed by a touchdown procedure (stepwise decrease of the annealing temperature for the amplification primers). To produce the cDNA, total RNA was reverse transcribed using the first-strand cDNA synthesis kit for RT-PCR (Roche) with random hexamers as primers, according to the manufacturer's recommendations. (B) To generate standard curves, template dilution series (cDNA mixture in four subsequent 1:50 dilution steps) were added to the reaction mixture. Results were processed using the LightCycler software package (version 3.5.28). The crossing points (CP) are indicated.

pressed in three or four transcripts of different sizes (5), differed significantly compared to ERK1c/ERK1 levels in normal human tissue and in human tumor cell lines. Interestingly, ERK1c/ERK1 mRNA levels were elevated in human tumors compared to the normal tissue counterpart, indicating a potential role of these isoforms in neoplastic growth.

The similar migration positions of ERK1c and ERK1 mRNAs (Fig. 2) and the lack of an ERK1-specific probe that cannot recognize ERK1c prevented estimates of the relative amount of ERK1c mRNA by Northern blotting. Therefore, we resorted to an LightCycler (real-time PCR)-based approach and designed specific probes for each one of the ERK1 spliced forms. Thus, the amplification was achieved by using forward primers located either within the ERK1c insert or, in the case of ERK1, spanning the exon 7/exon 8 boundaries and using harsh primer annealing conditions. Gel electrophoresis of the LightCycler amplification products confirmed the presence of only one amplicon in each case (data not shown). Standard curves of both reactions revealed equal amplification efficiencies (expressed as a slope) (Fig. 3A), allowing direct comparison of the crossing points of amplification. The difference between the crossing points was 2.86 in MCF-7 cells and 4.06 in HeLa cells, translating to 8.1- and 11.5-fold-higher expression of ERK1 compared to that of ERK1c (Fig. 3B). It should

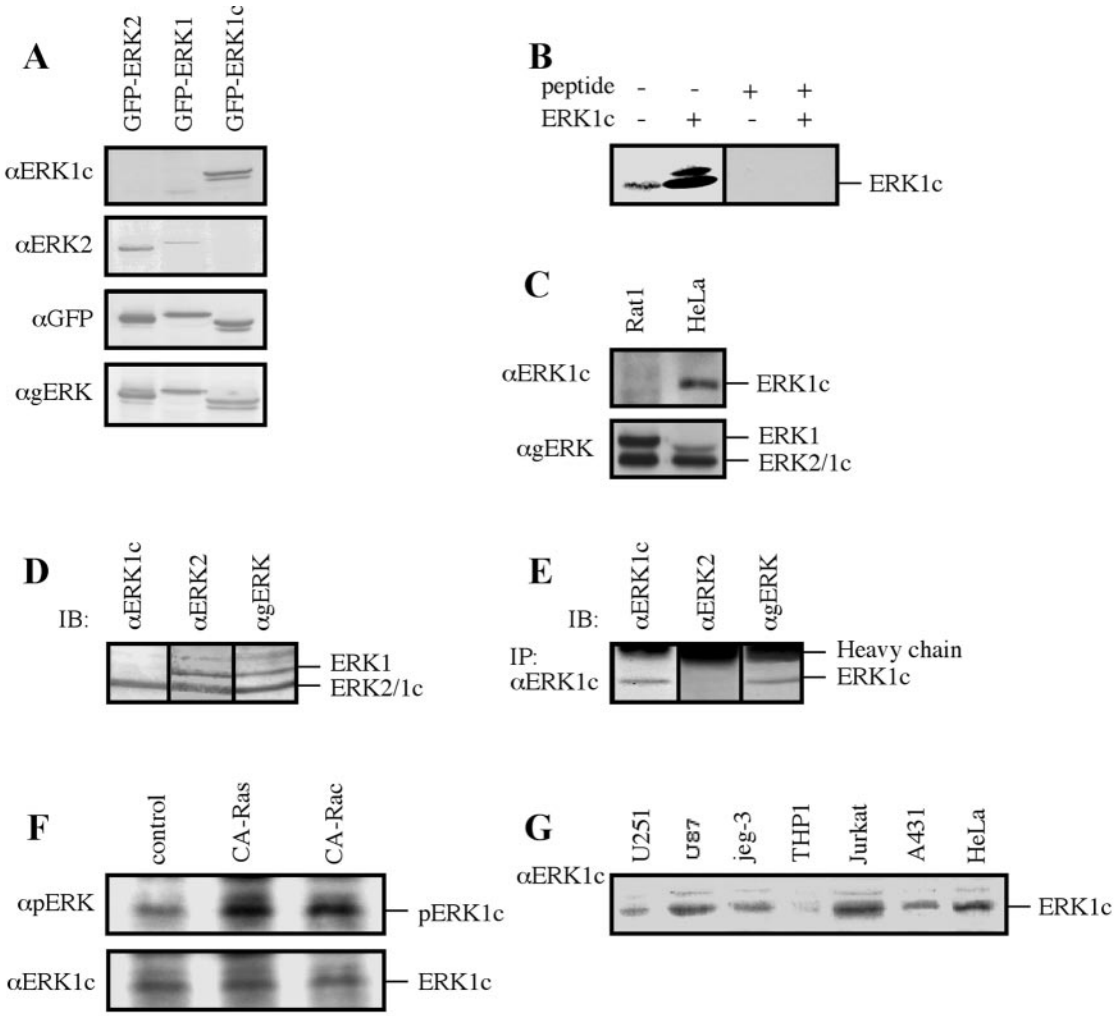

FIG. 4. Characterization of the endogenous ERK1c protein. (A) Testing the specificity of the anti-ERK1c Ab. HEK-293 cells were transfected with the indicated constructs, and extracts (containing cytosolic and nuclear proteins; 50 μg) were immunoblotted with four different Abs: anti-ERK1c Ab (αERK1c), anti-ERK2 Ab (αERK2), anti-GFP Ab (αGFP), or anti-ERK1/2 Ab (αgERK). (B) Competing the anti-ERK1c Ab with the antigenic peptide. HeLa cell extract (containing cytosolic and nuclear proteins; 50 μg) from nonstimulated HeLa cells transfected with ERK1c (+) or not transfected (−) were subjected to immunoblotting with anti-ERK1c Ab (ERK1c) in the absence (−) or presence (+) of the antigenic peptide (25 μg/ml). (C) ERK1c is not expressed in rat cells. HeLa and Rat1 cell extracts (50 μg) were loaded on SDS-polyacrylamide gels and immunoblotted with the indicated Abs. (D) ERK1c migrates together with ERK2 on SDS-polyacrylamide gels. HeLa cell extracts were loaded on one lane (100 μg) of the SDS-polyacrylamide gel and transferred to a nitrocellulose membrane. After the transfer, the membrane was cut into three pieces, and each piece was immunoblotted (IB) with a different Ab as indicated. (E) Immunoprecipitation of ERK1c from HeLa cells. An anti-ERK1c Ab was used to immunoprecipitate (IP) ERK1c from HeLa cell extract (500 μg), followed by immunoblotting (IB) with the indicated Abs. (F) ERK1c is phosphorylated on its Thr and Tyr residues upon activation. HeLa cells were transfected with constitutively activated Ras (CA-Ras), constitutively activated Rac (CA-Rac), or a vector control. ERK1c was immunoprecipitated with the anti-ERK1c Ab and immunoblotted with anti-pERK and anti-ERK1c Abs. (G) ERK1c expression in several human tumor cell lines. Cell lysate (50 μg) from a nonstimulated human glioblastoma brain tumor cell line, U-251 MG, U87 PTEN-deficient glioma cells, human choriocarcinoma cell line jeg-3, a natural human monocytic cell line (THP1), Jurkat T lymphocytes, A431 epidermal carcinoma cells, or HeLa cells were subjected to immunoblotting with anti-ERK1c Ab. The amounts of ERK1 and ERK2 detected in this experiment by anti-ERK Ab were similar in all cells. The experiments were reproduced three times.

be noted that in view of the high expression of ERK1 in cells, the estimated amount of ERK1c is considerable and roughly equals the amount of JNK1 in these cells (data not shown).

Expression and phosphorylation of endogenous ERK1c protein. Although the above results clearly indicate that ERK1c mRNA is expressed at considerable levels in various cell lines, it was not clear whether this is accompanied by a significant expression of the ERK1c protein. To study the ERK1c protein, we used the unique 18-amino-acid sequence of ERK1c to raise a specific polyclonal Ab against this protein. An immunoblot analysis revealed that the Ab raised is specific to ERK1c, as it failed to recognize GFP-tagged ERK1 (GFP-ERK1) or GFP-ERK2 and it did not detect a large number of cytosolic proteins in the extract (Fig. 4A). In addition, the Ab also detected an endogenous 42-kDa protein that migrated similarly to the exogenous ERK1c on SDS-polyacrylamide gels (Fig. 4B) and completely disappeared when the antigenic peptide was added to the Ab during the immunoblotting procedure. As expected,

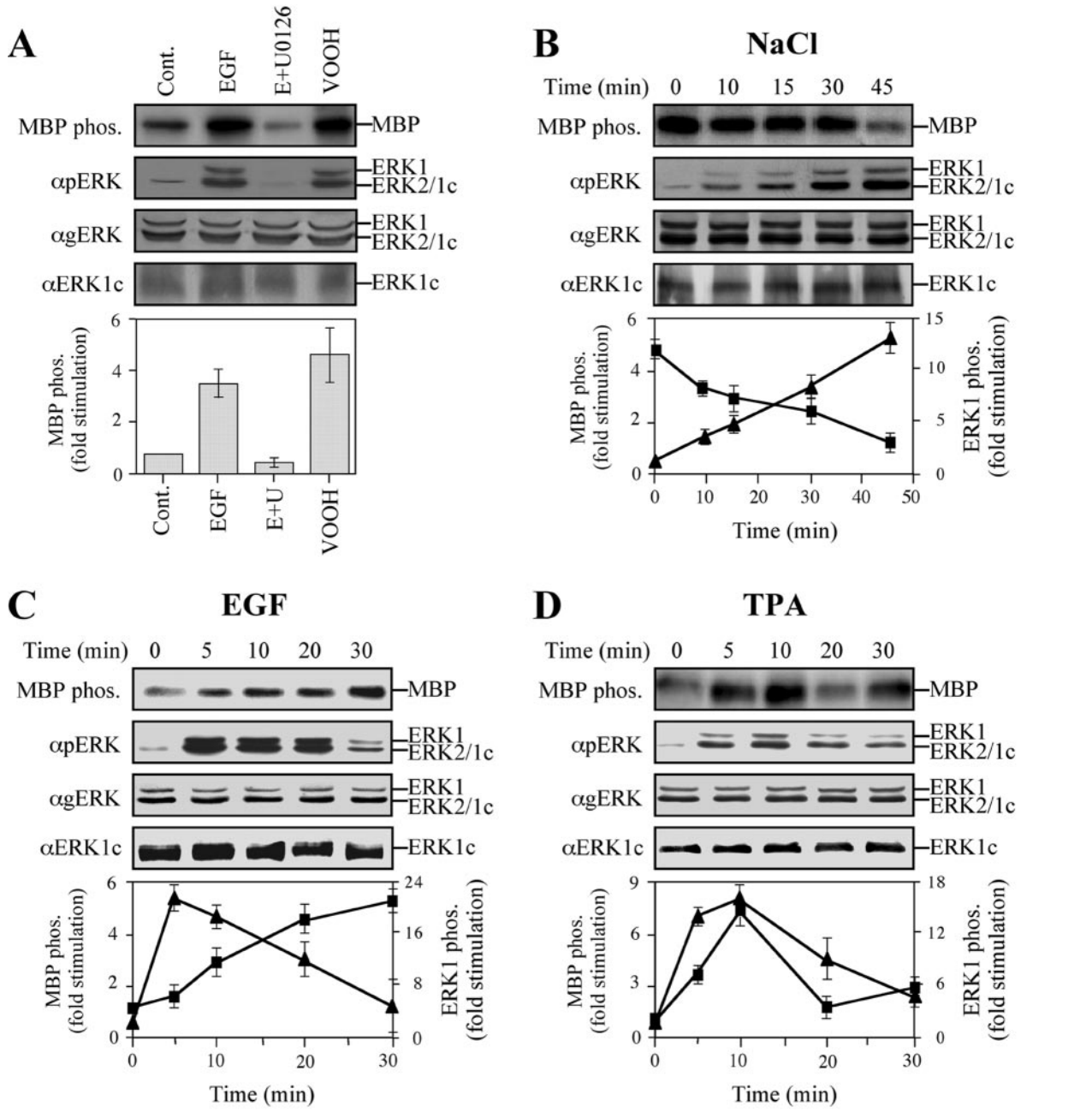

FIG. 5. (A) Kinetics of ERK1c activation. Stimulation and inhibition of MBP phosphorylation (MBP phos.) by ERK1c are shown. HeLa cells were serum starved for 16 h and then stimulated with either EGF (50 ng/ml, 10 min), EGF plus U0126 (E+U) (15-min pretreatment with 5 μM U0126, followed by 10 min of EGF [50 ng/ml]), or VOOH (100 μM Na_3VO_4 and 200 μM H_2O_2, 15 min) or left untreated as a control (Cont.). After harvesting, extracts were either immunoprecipitated with anti-ERK1c Ab (αERK1c) and subjected to an in vitro MBP phosphorylation (MBP phos.), or they were immunoblotted with anti-ERK1c, anti-pERK, or anti-gERK Ab. The bar graph shows the means ± standard errors (error bars) from three different experiments. (B) Time course of ERK1c activation by osmotic shock. HeLa cells were serum starved for 16 h and then stimulated with 0.7 M NaCl for the indicated times. ERK1c activity was examined and immunoblotting was performed as described above for panel A. Squares represent ERK1c activity, while the triangles represent the phosphorylation (phos.) of ERK1 and ERK2. The results in the graph show the means ± standard errors from three different experiments. (C and D) Time course of ERK1c activation by EGF and TPA. HeLa cells were treated as described above for panel B, except that EGF (50 ng/ml) or TPA (250 nM) was used for stimulation.

the 42-kDa band was detected in human cell lines, such as HeLa cells, but not in rat cells (Rat1 [Fig. 4C]).

Interestingly, immunoblots with anti-ERK1c, anti-ERK2, and anti-gERK Abs revealed that ERK1c migrates to exactly the same position as ERK2 in 10% polyacrylamide gels (Fig. 4D) and 12% polyacrylamide gels (not shown). This may complicate the detection of ERK1c-specific phosphorylation with anti-pERK Ab. To solve this problem, it became necessary to separate the two ERKs using the developed anti-ERK1c Ab. Indeed, we found that the Ab specifically immunoprecipitated

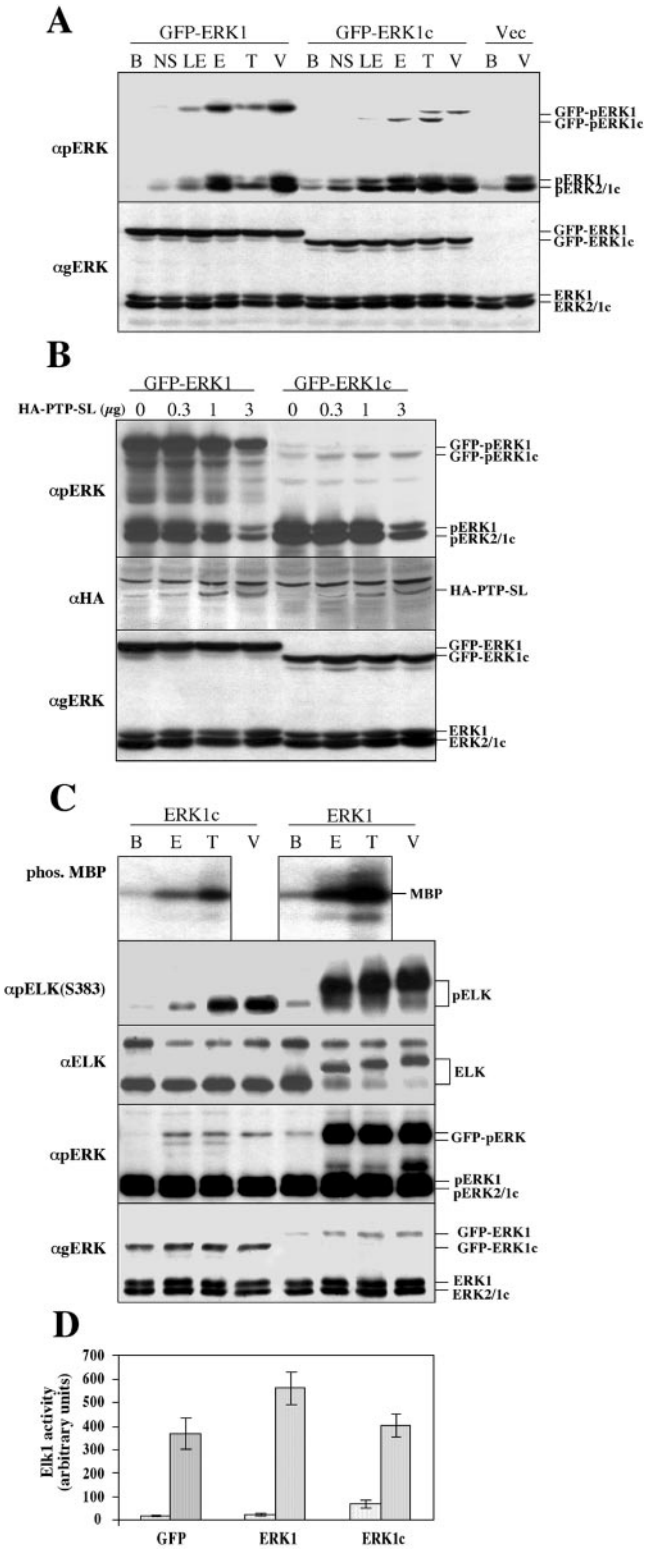

FIG. 6. Biochemical properties of ERK1c. (A) Phosphorylation of exogenous ERK1c in response to extracellular stimuli. COS7 cells were transfected with GFP-ERK1 or GFP-ERK1c. Two days later, the cells were either not starved (NS) or the cells were starved and stimulated with either EGF for 14 h (10 ng/ml, 12 h) (LE), EGF (50 ng/ml, 10 min) (E), TPA (250 nM, 15 min) (T), VOOH (Na_3VO_4 [100 μM] and H_2O_2 [200 μM], 20 min) (V), or left untreated (B) as control. Cell extracts were analyzed by immunoblotting with the indicated Abs. The data are from a representative experiment (the experiment was performed three times). (B) Differential dephosphorylation of ERK1 and ERK1c by PTP-SL. COS7 cells were cotransfected with plasmids (1 μg each) containing either HA-ERK1 or HA-ERK1c, together with the indicated amounts of plasmid containing wild-type PTP-SL. After serum starvation, the cells were stimulated with EGF (50 ng/ml, 10 min) and harvested. Cytosolic extracts were subjected to an immunoblot analysis with the indicated Abs (anti-HA Ab [αHA] used to demonstrate increasing PTP-SL). The data are from a representative experiment (the experiment was three times). (C) Phosphorylation of MBP and Elk1 by ERK1c. COS7 cells were transfected with GFP-ERK1 or GFP-ERK1c. After serum starvation, the cells were stimulated with EGF (50 ng/ml, 10 min) (E), TPA (250 nM, 15 min) (T), or VOOH (18 min) (V) or left untreated (B). The GFP-ERKs were immunoprecipitated with anti-GFP Ab and subjected to an in vitro kinase assay with MBP or Elk1 as the substrate. The phosphorylation (phos.) of MBP was detected by autoradiography on an X-ray film (Agfa). The phosphorylation of Elk1 was detected by anti-pElk1(S383) Ab and also by upshift of Elk1 detected by anti-Elk1 Ab. The phosphorylation and amount of the GFP-ERKs were determined by an immunoblot analysis with the indicated Abs. The positions of phospho-MBP (pMBP), GFP-ERKs, GFP-phospho-ERKs (GFP-pERKs), and Abs are indicated at the sides of the gels. These results were from a representative experiment (the experiment was performed four times). (D) Effect of ERK1c on Elk1 transcriptional activity. HEK-293 cells were transfected with pFR-Luc (reporter), pFA2-Elk1 (fusion transactivator), pRenilla (reporter of transfection yield), together with GFP-ERK1 (ERK1), GFP-ERK1c (ERK1c), or GFP empty vector. Serum-starved cells were stimulated with EGF (50 ng/ml) for 14 h. Luciferase and *Renilla* luminescence were monitored as described in Materials and Methods. The results represent the means and standard errors (error bars) of three experiments.

ERK1c but not ERK1 or ERK2 (Fig. 4E), supporting their specificity. By using immunoprecipitation, followed by immunoblotting with anti-pERK Ab (46), we detected considerable ERK1c phosphorylation in serum-starved, vector-transfected HeLa cells, which increased significantly upon expression of V12-Ras or V12-Rac in the cells (Fig. 4F). Finally, immunoblot analysis with the developed Ab revealed that ERK1c is expressed at various levels in a battery of human cells (Fig. 4G). The amount of ERK1c expressed is the highest in Jurkat cells, followed by HeLa and U87 cells. These results suggest that like rat ERK1b (3, 47, 48), ERK1c is also expressed differently in different cell lines and conditions.

ERK1c activation is MEK dependent but has different kinetics than ERK1 activation. The existence of considerable levels of ERK1c in various cells led us to study whether the basal and stimulated ERK1c activities are similar to those of the other ERKs. Thus, serum-starved HeLa cells were treated with various agents, and ERK1c activity was determined by immunoprecipitation, followed by an in vitro kinase assay using MBP as a substrate. Fold activation or inhibition of ERK1c was compared to that of ERK1, as estimated by its degree of double phosphorylation, which directly reflects its degree of activity (46). It should be noted that the doubly phosphorylated ERKs at 42 kDa are probably composed of phosphorylated ERK2 and phosphorylated ERK1c, so it cannot be used to determine the activity of each one alone. As shown above, ERK1c demonstrated a relatively high level of basal activity compared to the very low activity of ERK1 under these conditions (Fig. 5A; also see Fig. S11 in the supplemental material). EGF stimulated the activity of ERK1c about 3.5-fold over the basal level; this activation was aborted by pretreatment of the cells with the MEK inhibitor U0126. Moreover, incubation

with U0126 resulted in reduction of the activity to a level lower than that of ERK1c from untreated cells, indicating that the high basal activity is also dependent on MEK. The general ERK activator peroxovanadate that served as a positive control induced the activity of ERK1c to an extent similar to that induced by EGF.

We then examined the time course of ERK activation by various stimuli. We found that the addition of 0.7 M NaCl, which causes osmotic stress, resulted in a continuous inactivation of ERK1c for up to 45 min after treatment (Fig. 5B). This was in sharp contrast to the activation of ERK1 under these conditions, which was continuously elevated over the examined time period. Different activation kinetics were also detected upon stimulation with EGF, which caused a constant elevation of ERK1c activity for up to 30 min of stimulation, while the activation of ERK1 peaked 5 min after stimulation, stayed high at 20 min, and dropped at 30 min (Fig. 5C). Finally, the time course of activation by TPA consistently revealed two phases of activation, with a peak at 10 min, reduction of activity at 20 min, and then an increase at 30 min after stimulation (Fig. 5D). ERK1 activity under these conditions peaked at 10 min after stimulation and declined thereafter. Taken together, the results indicate that the kinetics of ERK1c activation and inactivation are distinct from those of ERK1. It should be noted that ERK1 did not exhibit any detectable basal activity (Fig. 5), which also holds true for ERK2 (data not shown). Therefore, it is likely that the pERK detected at 42 kDa is, at least in part, related to the phosphorylation of ERK1c, indicating that the specific activity of ERK1c in resting cells might be much higher than that of ERK1 and ERK2.

Phosphorylation and dephosphorylation of recombinant ERK1c. The differences in the kinetics of activation of ERK1c and ERK1 by extracellular agents prompted us to characterize the activation and inactivation processes of ERK1c in detail compared to those of ERK1 and ERK1b. Since the expression levels of ERK1c are lower than those of ERK1 and ERK2, we first compared the ability of ectopically expressed ERK1c to undergo phosphorylation in response to extracellular stimuli to that of a similar amount of ectopically expressed ERK1. To this end, COS7 cells were transfected with human GFP-ERK1 or GFP-ERK1c, serum starved, treated with EGF, TPA, or peroxovanadate, and subjected to an immunoblot analysis with anti-pERK and anti-gERK Abs. We found that although GFP-ERK1c is doubly phosphorylated in response to stimulation by EGF, TPA, or pervanadate, this phosphorylation is significantly lower than that of GFP-ERK1 (Fig. 6A). Interestingly, two forms of phosphorylated GFP-ERK1c were recognized; the lower one migrated with the nonphosphorylated protein, while the upper one was probably formed due to some sort of posttranslational modification. The upper band was recognized by the anti-pERK Ab but not by the anti-gERK Ab, probably due to the small amount of this form and the lower sensitivity of the anti-gERK Ab. Alternatively, it is possible that the additional modification of the upper form of ERK1c interferes with the recognition by the anti-gERK Ab. It was also noticed that the activities of the endogenous ERKs were higher in the cells transfected with ERK1c than in the cells transfected with ERK1. An explanation for this effect could be interference of ERK1c with the inhibition of exchange factors upstream of the ERK cascades, a process that is known to play a role in the down-regulation of the ERK cascade (21).

The most notable difference between the rat ERK1b and ERK1 proteins is the resistance of ERK1b to phosphatase activity as a result of reduced binding (47). To determine whether ERK1c is also resistant to phosphatases, we cotransfected COS7 cells with either GFP-ERK1c or GFP-ERK1 together with increasing amounts of HA-PTP-SL, a tyrosine phosphatase that was shown to bind and dephosphorylate ERK1 and ERK2 (27). The cells were then stimulated with TPA for 15 min, and the phosphorylation was assessed by immunoblotting with anti-pERK Ab. While GFP-ERK1 and endogenous ERK1 and ERK2 were all gradually dephosphorylated with the increasing amount of transfected HA-PTP-SL, the phosphorylation of the lower band of GFP-ERK1c increased, while the phosphorylation of the upper band formed decreased, resulting in an unchanged amount of total phosphorylated GFP-ERK1c by elevating PTP-SL expression (Fig. 6B). These results best fit a model where the phosphates that induce the retardation in mobility in the gel, but not the TEY phosphates, are sensitive to PTP-SL action. Removal of the retarding phosphates causes the faster migration of the molecules, causing the elevated amount of TEY-phosphorylated faster-migrating GFP-ERK1c detected in the figure.

Phosphorylation of MBP and Elk1 by ERK1c. In our previous studies (47), we found that rat ERK1b phosphorylates Elk1 differently than ERK1. To determine the ERK1c activity and substrate specificity, COS7 cells were transfected with either GFP-ERK1 or GFP-ERK1c, starved, and stimulated with different extracellular agents. The GFP molecules were immunoprecipitated, washed extensively, and subjected to an in vitro kinase assay using MBP as a general substrate and Elk1 as a known physiological substrate of ERKs (12). Thus, the stimulated activity of ERK1c toward MBP (Fig. 6C) was smaller than that observed with ERK1, which correlated nicely with the signal of anti-pERK Ab. The phosphate incorporation into the regulatory S383 of Elk1 was induced upon phosphorylation of ERK1c as detected by staining with anti-pElk1(S383) Ab (Fig. 6C), but phosphorylation by ERK1c could not cause the appearance of higher Elk1 bands on the gel as the phosphorylation by ERK1 did (Fig. 6C). The inability of ERK1c to cause Elk1 shift is probably the result of lower activity of ERK1c, but it may also be due to phosphorylation of fewer sites on Elk1, which might be caused by different substrate specificities, as was shown for rat ERK1b (47).

We also examined the effect of ERK1c overexpression on the activity of Elk1 in HEK-293 cells and found that ERK1c induced high basal Elk1 transcriptional activity probably due to its lack of sensitivity to phosphatases (Fig. 6D). On the other hand, overexpression of ERK1c increased the EGF-stimulated activity of Elk1, but to a lower level than the one induced by ERK1 (Fig. 6D), corroborating the decreased phosphorylation of Elk1 by ERK1c compared to its phosphorylation by ERK1. Taken together, our results indicate that the rate of ERK1c activation by MEKs or other kinases is lower than the rate of ERK1 activation. However, once phosphorylated on its TEY motif, ERK1c is an efficient protein kinase that phosphorylates at least some of the substrates of ERK1 or ERK2 and can induce activation of Elk1.

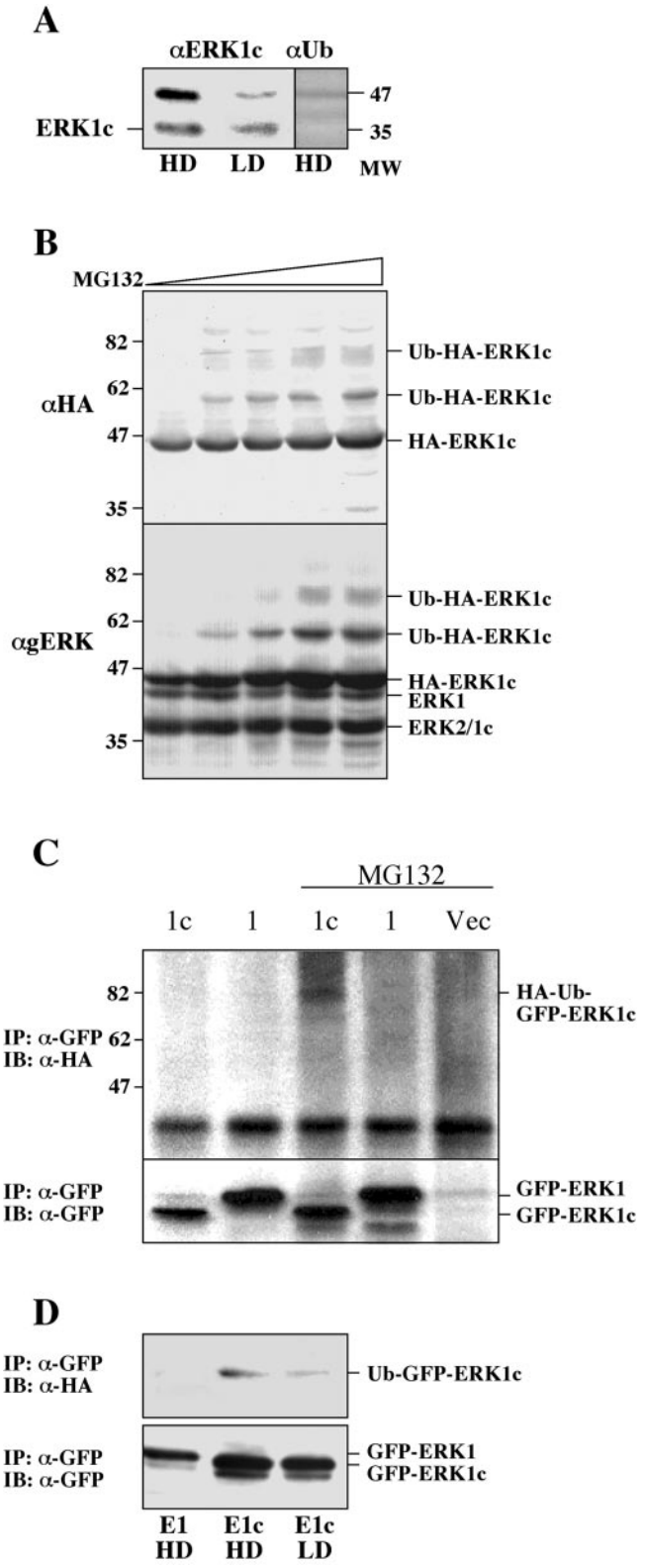

FIG. 7. Monoubiquitination of ERK1c. (A) Appearance of a 50-kDa ERK1c protein in dense cells. HeLa cells were grown until they were confluent and either harvested (medium density) or left for another 36 h (high density [HD]) and then harvested. Cell extracts (100 μg) were subjected to immunoblotting with the indicated Abs. These results were from a representative experiment (the experiment was performed five times). In parallel, ERK1c from the high-density cell extracts was purified on MonoQ, heparin, and Superdex columns. An aliquot of the purified ERK1c was immunoblotted with antiubiquitin Ab (αUb). MW, molecular weight in thousands. (B) Appearance of putative mono- and diubiquitinated ERK1c upon MG132 treatment. HeLa cells were transfected with HA-ERK1c. Forty-eight hours later, the cells were treated with MG132 (0, 0.1, 0.3, 1.0, and 3 μg/ml) for 8 h, and the expression of HA-ERK1c and endogenous ERKs was tested by immunoblotting with the indicated Abs. These results were from a representative experiment (the experiment was performed two times). (C) Monoubiquitination of GFP-ERK1c but not ERK1c in response to treatment with MG132. COS7 cells were cotransfected with HA-ubiquitin and GFP constructs of ERK1 (lanes 1) or ERK1c (1c) or vector (Vec) alone. After 2 days, the cells were treated with MG132 (1 μg/ml, 12 h) or left untreated, and the GFP proteins were immunoprecipitated (IP) by anti-GFP Ab (α-GFP). The amounts of GFP-containing proteins and HA-ubiquitin were analyzed by immunoblotting (IB) with anti-GFP or anti-HA Ab. The positions of GFP-ERK1, GFP-ERK1c, and HA-ubiquitin bound to GFP-ERK1c (HA-ERK1c) are indicated. These results were reproduced three times. (D) Immunoprecipitation of HA-ubiquitinated GFP-ERK1c from cells at different densities. HeLa cells were cotransected with GFP-ERK1c or GFP-ERK1 together with HA-ubiquitin (HA-Ub) and grown at low and high densities as described above. GFP-ERK1 containing cells were grown at high density. The cells were then harvested, and cell lysates were subjected to immunoprecipitation (IP) with monoclonal anti-GFP Ab. HA-ubiquitin and GFP-ERKs were detected by Western blotting (IB) with the appropriate Ab.

Monoubiquitination of ERK1c. We have noticed that beside the 42-kDa band that was routinely recognized by the anti-ERK1c Ab, elevated cell density often resulted in the recognition of another protein band at about 50 kDa (Fig. 7A). This band was also recognized by anti-gERK Ab and competed out by the antigenic peptide (not shown), indicating that it is indeed a modified form of ERK1c. The 8-kDa difference raised the possibility that the 50-kDa band is a monoubiquitinated ERK1c, and indeed a band with a similar molecular mass was recognized by antiubiquitin Ab in a purified ERK1c fraction (Fig. 7A). At this time, monoubiquitination has not been reported to play a role in the regulation of the ERK cascade, and polyubiquitination seems to play a role only under extreme conditions (22). However, the recognition of a 50-kDa band that may represent a monoubiquitinated ERK1c prompted us to examine the possible role of ubiquitination in the regulation of ERK1c expression. To this end, we used increasing concentrations of proteosome inhibitor MG132 added to HA-ERK1c-transfected COS7 cells and monitored the expression levels of ERK1c. We found that this treatment with MG132 had only a small effect on the expression of HA-ERK1c and as expected, on the expression of endogenous ERK1 and ERK2. Moreover, no evidence for polyubiquitination was observed under any of the conditions used, indicating that ERK1c, as well as ERK1 and ERK2, is not significantly regulated by the ubiquitin-proteosome system. On the other hand, two higher-molecular-mass bands were recognized by both anti-HA and anti-gERK Abs. The first band was 8 kDa higher than the HA-ERK1c band, and another band 16 kDa higher was also detected, which suggests that HA-ERK1c may undergo monoubiquitination and perhaps also diubiquitination under certain conditions.

To confirm that ERK1c is monoubiquitinated, we examined whether ubiquitin can specifically bind ERK1c. COS7 cells were cotransfected with HA-ubiquitin together with GFP-ERK1c, GFP-ERK1, or empty vector, followed by treatment

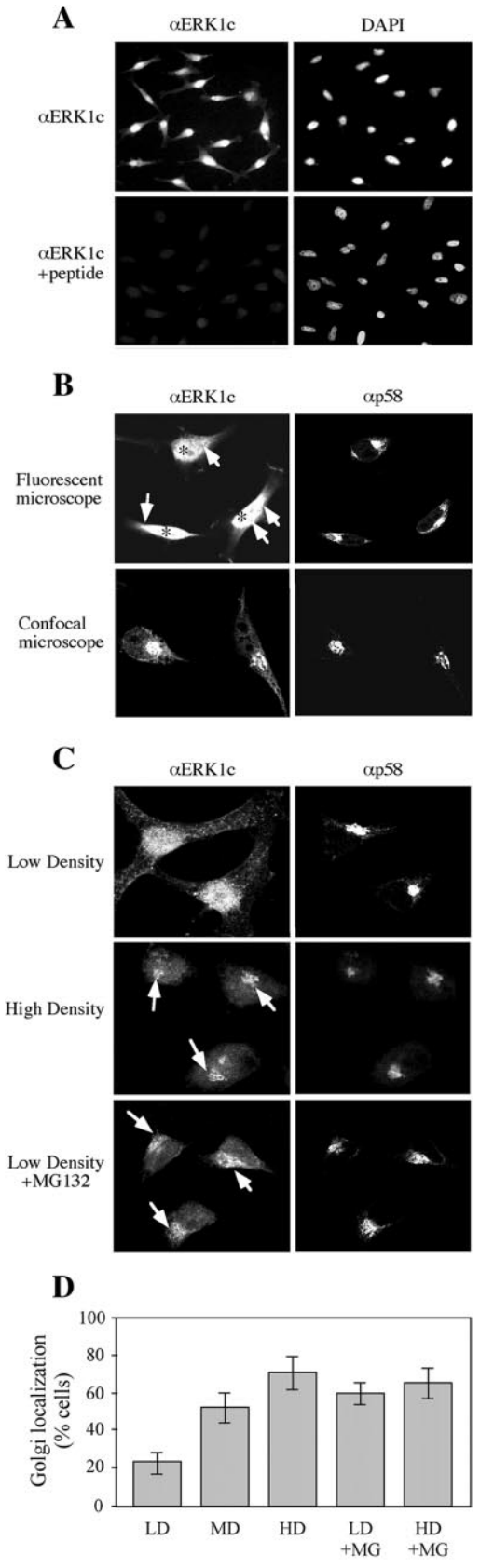

with MG132. The GFP molecules were then immunoprecipitated, and the presence of ubiquitinated molecule in the precipitate was tested by immunoblotting with anti-HA Ab. In the MG132-treated cells, the expression of GFP-ERK1c and GFP-ERK1 was not changed significantly, but immunoblotting with an anti-HA Ab showed one band at ~75 kDa only in the cells transfected with GFP-ERK1c (Fig. 7C). The migration of the HA band corresponds to the expected mass of GFP-ERK1c (65 kDa) together with one ubiquitin molecule. No higher-molecular-mass ERK1c was detected, again indicating that ERK1c is not regulated by polyubiquitination. As expected, ERK1 was not modified by ubiquitin under these conditions, emphasizing that monoubiquitination is specific to ERK1c.

Since we showed above that the amount of a putative monoubiquitinated 50-kDa ERK1c is increased in dense cells (Fig. 7A), it was important to examine whether the monoubiquitination process of ERK1c is also enhanced in dense cells. Therefore, HeLa cells were cotransfected with HA-ubiquitin together with GFP-ERK1c or GFP-ERK1, and then the cells were grown to either low or high densities. The presence of ubiquitinated molecules was tested by immunoprecipitation with anti-GFP Ab, followed by immunoblotting with anti-HA Ab. As expected, the HA-labeled band at 75 kDa (monoubiquitinated ERK1c) was most abundant in the high-density, ERK1c-transfected cells, weaker in low-density cells, and not detected at all in high-density, ERK1-transfected cells (Fig. 7D). Taken together, the results indicate that ERK1c is regulated by monoubiquitination and that this process is enhanced by various cellular conditions, such as increased cell density or proteosome inhibition. Since monoubiquitination plays a role in the sorting mechanisms of various molecules (16, 36), it is

FIG. 8. Immunostaining of ERK1c. (A) Subcellular localization of ERK1c. HeLa cells were grown on 18-mm microslides in 12-well plates for 24 h. The cells were stained with anti-ERK1c Ab (αERK1c) and DAPI as described in Materials and Methods. The specificity of staining was confirmed by competition with the antigenic peptide (25 μg/ml). (B) ERK1c is localized in the nucleus and Golgi apparatus. HeLa cells were stained as described above with anti-ERK1c and anti-p58 Abs. Visualization with a regular fluorescence microscope revealed nuclear staining (asterisks) and perinuclear staining (arrows) that corresponded to the Golgi staining. With a confocal microscope, we detected sections in which only the Golgi staining by anti-ERK1c and anti-p58 Abs was apparent. (C) Staining of ERK1c in cells at different densities or MG132-treated cell cultures. HeLa cells (20,000 cells/well in the Low Density panels and 120,000 cells/well in the High Density panel) were seeded on 18-mm microslides in 12-well plates. Twenty-four hours after plating, the cells were either treated with MG132 (1 μg/ml, 6 h) or left untreated and then were fixed and stained with anti-ERK1c and anti-p58 Abs. The staining was visualized with a confocal microscope as described above for panel B. The positions of the Golgi apparatus in the stained cells are indicated by the white arrows. (D) Accumulation of ERK1c in the Golgi apparatus is dependent on cell density. HeLa cells were grown at three different densities: 20,000 cells/well (low density [LD]), 60,000 cells/well (medium density [MD]), and 120,000 cells/well (high density [HD]). HeLa cells were seeded on 18-mm microslides (in 12-well plates), which were treated as described in the legend to Fig. 8C. The percentage of cells with apparent Golgi localization of ERK1c was determined by counting 200 cells in each slide. The values are the means ± standard errors (error bars) for three experiments.

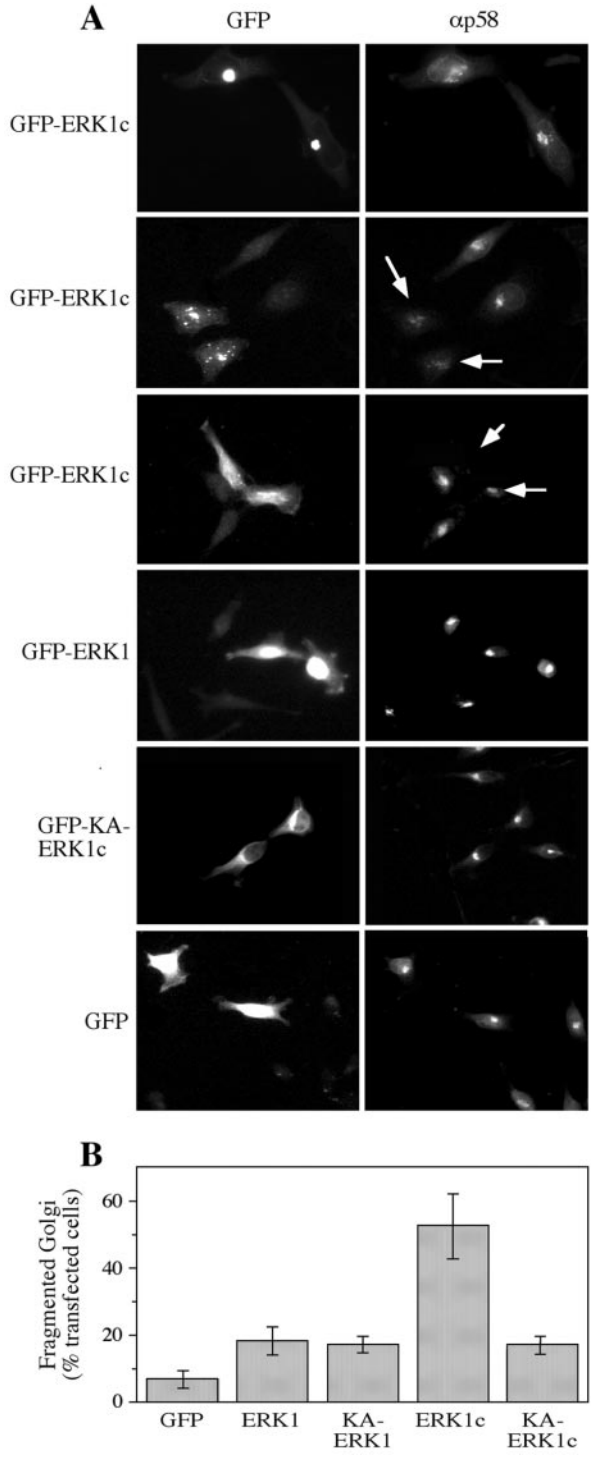

FIG. 9. Overexpression of GFP-ERK1c results in Golgi fragmentation. (A) Localization and effect on Golgi apparatus of the GFP-ERK constructs. HeLa cells were transfected with GFP-ERK1c, GFP-ERK1, GFP-KA-ERK1c, or GFP and grown on microslides in 12-well plates. Fourteen hours after transfection, the cells were fixed and stained with anti-p58 Ab (αp58) and examined with a fluorescence microscope. Fragmentation or lack of Golgi apparatus is indicated by the white arrows. (B) Quantitation of Golgi fragmentation. The HeLa cells (200 cells in each slide) in panel A were counted, and the percentage of cells with fragmented Golgi apparatus out of cells expressing GFP-ERK1c is presented. The values are the means ± standard errors (error bars) for three experiments.

possible that this mechanism directs ERK1c to specific subcellular compartments.

Subcellular localization of ERK1c. Unlike ERK1 and ERK2 that are localized in the cytosol, we have previously shown that ERK1b is localized in nuclei of resting Rat1 cells (48). To determine whether ERK1c shares this feature, we studied its subcellular localization by immunostaining. Thus, staining of HeLa cells (Fig. 8A) and MCF7 cells (not shown) revealed that ERK1c is localized primarily in the nucleus, but it is also detected in some perinuclear regions (Fig. 8A). This staining was specific, since it was readily competed out by the Ab's antigenic peptide. Costaining the cells with the *cis*-Golgi apparatus marker p58 (18) revealed that the perinuclear region stained by the anti-ERK1c Ab is probably the Golgi apparatus (Fig. 8B, upper panel). This Golgi apparatus localization was confirmed by confocal microscopy by finding sections where the Golgi apparatus was clearly detected without the background of other stained organelles (Fig. 8B; also see Fig. S12 to S14 in the supplemental material). Thus, like ERK1b, ERK1c is not retained in the cytosol of resting cells and is directed mainly to the nucleus. However, unlike ERK1b, ERK1c appears to be localized also in the Golgi apparatus of these cells.

Since we found that ERK1c is modified by monoubiquitination in high-density and MG132-treated cells, we undertook to examine whether these cellular conditions are accompanied by changes in the subcellular localization of ERK1c. To do so, we plated HeLa cells in low, medium, and high densities in different plates. The cells were then either treated with MG132 for 6 h or left untreated, followed by staining with anti-ERK1c and anti-p58 Abs and visualization of Golgi apparatus-containing horizontal sections with a confocal microscope. We found that the number of cells containing ERK1c in the Golgi apparatus was higher in dense cells (Fig. 8C and D). MG132 increased the accumulation of ERK1c in the Golgi apparatus in low-density, but not in high-density cell cultures. Thus, the accumulation of ERK1c in the Golgi apparatus is indeed correlated with increased monoubiquitination, supporting the notion that monoubiquitination directs ERK1c to the Golgi apparatus.

Overexpressed ERK1c is localized in the Golgi apparatus and induces Golgi fragmentation. We then studied the distribution and function of ectopically expressed ERK1c. To do so, HeLa cells were transfected with GFP-ERK1c, grown at medium density for 14 h, fixed, and stained with anti-p58 Ab. Two main types of GFP distribution were observed (Fig. 9A), a spotted localization (~30%) and a diffuse distribution (~70%). The spotted distribution of GFP-ERK1c was concentrated in a discrete part of the perinuclear region of the cells. This was an organelle-like appearance that was either confined to one spot (~40% of the cells) (Fig. 9A, top left panel), or looked fragmented, with one main spot and speckles around it (~60% of the cells) (Fig. 9A, top right panel). In these cells, GFP-ERK1c was always located with the Golgi apparatus (top αp58 panel), and indeed in the cells containing the fragmented distribution of GFP-ERK1c, the Golgi apparatus appearance was also fragmented and weaker (second αp58 panel). It should be noted that the GFP-ERK1c distribution was usually more condensed than that of the Golgi marker (Fig. 9A; also see Fig. S15 in the supplemental mate-

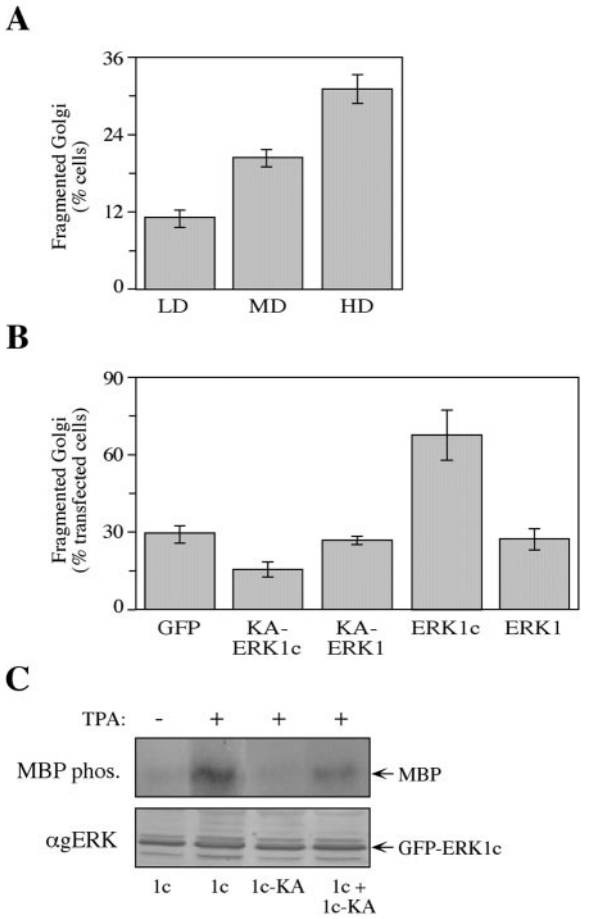

FIG. 10. Inhibition of cell density-dependent Golgi fragmentation by the dominant-negative KA-ERK1c. (A) Golgi fragmentation increased with elevated cell density. HeLa cells were seeded on 18-mm microslides at low density (LD) (20,000 cell/well of a 12-well plate), medium density (MD) (60,000 cells/well), and high density (HD) (120,000 cells/well). Twenty-four hours after plating, the cells were fixed and stained with anti-p58 Ab. The percentage of cells with fragmented Golgi apparatus was determined by counting 200 cells in each slide. The values are the means ± standard errors (error bars) for three experiments. (B) Overexpression of KA-ERK1c inhibits cell density-dependent Golgi fragmentation. HeLa cells were seeded on 18-mm microslides at high density (120,000 cells/well) and transfected with GFP, GFP-KA-ERK1c, GFP-KA-ERK1, GFP-ERK1c, or GFP-ERK1. Twenty-four hours after transfection, the cells were fixed and stained with anti-p58 Ab. The percentage of cells with fragmented Golgi apparatus out of cells expressing the exogenous construct is presented. The values are the means ± standard errors (error bars) for three experiments. (C) KA-ERK1c has a dominant-negative effect. HEK-293 cells were transfected with GFP-ERK1c (1c), GFP-KA-ERK1c (1c-KA), or HA-ERK1c together with GFP-KA-ERK1c (1c + 1c-KA). The cells were serum starved and stimulated with TPA (+) (250 nM, 15 min) or left untreated (−). After harvesting, the GFP proteins were immunoprecipitated with anti-GFP Ab, subjected to an in vitro MBP phosphorylation (MBP phos.) and concomitantly immunoblotted with anti-gERK Abs (αgERK) to confirm equal immunoprecipitation of the GFPs.

rial), suggesting that GFP-ERK1c, but not endogenous ERK1c, is localized in a specific part of the Golgi apparatus. Taken together, these results verify the ability of ERK1c to be localized in the Golgi apparatus of human cells.

Unlike the spotted distribution of GFP-ERK1c, the rest of the cells exhibited a diffuse GFP-ERK1c distribution all over the cell (Fig. 9, third GFP-ERK1c panel), and both these localizations of GFP-ERK1c were different from the nuclear localization of GFP-ERK1 (fourth GFP-ERK1c panels). The inactive GFP-KA-ERK1c, in which the lysine in the ATP binding site was replaced with alanine, was also localized in the Golgi apparatus but was detected in additional regions of the cytoplasm. Importantly, Golgi fragmentation or disappearance was detected not only in the cells with the spotted GFP-ERK1c appearance but also in ~50% of the cells in which GFP-ERK1c was diffusely distributed (third αp58 panel). Unlike wild-type GFP-ERK1c, GFP-KA-ERK1c did not lead to Golgi fragmentation, indicating that the ERK1c-induced Golgi fragmentation is dependent on its intact kinase activity. Overexpression of GFP-ERK1 and GFP alone did not influence Golgi fragmentation. Quantitation of the phenomenon (Fig. 9B) revealed that the percentage of cells with fragmented Golgi apparatus out of all transfected cells was threefold higher in cells overexpressing GFP-ERK1c than in cells overexpressing GFP-KA-ERK1c, GFP-ERK1, or GFP-KA-ERK1. These results clearly indicate that overexpressed ERK1c can induce Golgi fragmentation. As such, the results best fit a model in which GFP-ERK1c is produced in the cytosol, giving rise to its diffuse distribution in cells with intact Golgi apparatus. This is followed by an accumulation of ERK1c in the Golgi apparatus (a spot of GFP-ERK1c and intact Golgi apparatus), which leads first to fragmentation of the Golgi apparatus (speckles of GFP-ERK1c and fragmented Golgi apparatus) and then to its complete disappearance (diffuse ERK1c and no Golgi apparatus).

ERK1c regulates the cell density-induced Golgi fragmentation. Our results above clearly indicate that ERK1c can accumulate in the Golgi apparatus under some circumstances and that overexpression of exogenous ERK1c can induce Golgi fragmentation. Therefore, it was important to link the observations and examine whether accumulation of endogenous ERK1c in the Golgi apparatus is indeed required for Golgi fragmentation under the conditions examined. For this purpose, we first determined whether the accumulation of ERK1c in the Golgi apparatus of dense cells is accompanied by an increased Golgi fragmentation. To this end, we examined cultures with increasing cell density and found that the number of cells containing fragmented Golgi apparatus is indeed correlated with the cell density (Fig. 10A). This is the first description of cell density-dependent Golgi fragmentation, although the role of this phenomenon is not clear.

We then examined whether ERK1c may be involved in this cell density-induced Golgi fragmentation. To do so, we overexpressed the inactive GFP-KA-ERK1c construct in high-density HeLa cells and found that it reduced the amount of Golgi fragmentation by 50% (Fig. 10B, compare GFP and KA-ERK1c). This reduction was probably due to the dominant-negative effect of the inactive GFP-KA-ERK1c on the endogenous ERK1c, which is demonstrated in Fig. 10C. The dominant-negative effect of GFP-KA-ERK1c was specific to the fragmentation induced by elevated cell density, as there was no reduction in Golgi fragmentation in low-density KA-ERK1c-expressing cells (Fig. 9C). Moreover, the cell density-induced Golgi fragmentation was mediated specifically by ERK1c, as GFP-ERK1 or GFP-KA-ERK1 had no effect on

this process. Moreover, overexpression of ERK1c in dense cells induced more Golgi fragmentation than in the medium-density cells shown in Fig. 9B. Taken together, our results clearly demonstrate that ERK1c not only accumulates in the Golgi apparatus of confluent cells but that this accumulation is required for enhanced Golgi fragmentation in these cells.

DISCUSSION

In this manuscript, we describe for the first time ERK1c, which seems to be an ortholog of the previously identified ERK1b (48). Both proteins are the products of an alternative splicing event that incorporates the intron between exon 7 and exon 8 (intron 7) of ERK1 into ERK1 mRNA. Indeed, the two proteins share several features, including a kinase domain, activation loop, and a somewhat disrupted regulatory CRS/CD domain. These similarities contribute to similar substrate specificities, which are somewhat different from the specificities of ERK1 and ERK2, and to a similar lack of sensitivity to phosphatases compared to those of ERK1 and ERK2.

However, despite their considerable similarities, the differences in the structure of ERK1b and ERK1c are reflected in several distinct properties. One obvious difference that is caused by the distinct inserted introns is the molecular mass of the proteins. ERK1c contains a 18-amino-acid stretch that replaces the C terminus of ERK1, resulting in a 40-kDa protein that migrates to 42 kDa on SDS-polyacrylamide gels. ERK1b contains a 26-amino-acid insert followed by the original C terminus of ERK1, resulting in a 46-kDa protein. An additional difference between the proteins is their phosphorylation by MEK1. While the kinetics of phosphorylation of ERK1b by MEK1 is similar to that of ERK1 and ERK2, the phosphorylation of ERK1c by MEK1 is much slower (Fig. 6). These differences and the relative resistance to phosphatases are reflected in different kinetics of activation (Fig. 5). Since ERK1c can be phosphorylated and activated by conditions that do not allow phosphorylation of ERK1 and ERK2, it is possible that its regulation is mediated by different enzymes, besides MEK-independent mechanisms. Unlike ERK1 and ERK2, the spliced forms ERK1b and ERK1c are localized in the nuclei of resting cells. However, only ERK1c can be monoubiquitinated, a process that seems to cause its localization in the Golgi apparatus under various cellular conditions. Moreover, we clearly show here that ERK1c has a unique physiological role in the regulation of Golgi fragmentation, which is not shared by ERK1.

Thus, we show that the ERK1 gene can give rise to at least two proteins (ERK1 and ERK1b in rodents; ERK1 and ERK1c in primates) with diverse molecular properties and different functions under distinct cellular conditions. Generally, these types of alternative splicing processes may broaden the battery of substrates and conditions under which the ERK cascade can operate, and thus, it can extend the signaling specificity of the cascade. In addition, these types of alternative splicing may contribute a great deal to the differences between species, which occur despite the similarities in their gene contents and sequences.

The differences between ERK1b and ERK1c may also emphasize the importance of the C-terminal tail of ERKs for their functions. We have previously shown that interference with the regulatory C-terminal region of ERK1, not the actual sequence of the 26-amino-acid insert, is important for the different properties of ERK1b (47). Similarly, many of the differences observed for ERK1c may be due to the short C terminus and not necessarily due to the actual sequence of its C-terminal 18-amino-acid tail. One structure-function aspect that is apparent by the altered C terminus is the reduced sensitivity of both ERK1b and ERK1c to phosphatases. It has previously been shown that the CRS/CD domain, and in particular Asn 339, are essential for the recognition of ERK1 by various phosphatases (2, 38, 42). However, despite the existence of an intact CRS/CD region in the sequences of both ERK1b and ERK1c, they were not properly recognized by PTP-SL and other MAPK phosphatases. Therefore, it would seem that the CRS/CD region is important but not sufficient for this recognition. Reasons for the lack of sensitivity to phosphatases include a requirement for an additional sequence at a proper distance in ERK1 or sequestration of the CRS/CD domain by the unique insert sequences of ERK1b and ERK1c. However, since several mutations in these regions are less sensitive to phosphatases as well (47; also data not shown), the most likely explanation for this lack of recognition is the lack of proper conformation, which is significantly modified in ERK1b and ERK1c compared to ERK1.

Another functional aspect that is modified in ERK1b and ERK1c is their interaction with the upstream activators (MEKs). We have previously demonstrated that ERK1b does not interact properly with MEK1, which induced nuclear localization of ERK1b, but did not significantly alter ERK1b activation (47). This result may suggest that the two functions of MEKs, namely, cytosolic retention and activation, may be exerted by interaction with different regions in ERK1. The facts that ERK1c exhibits a reduced interaction (data not shown) and reduced activation by MEKs (Fig. 6) may indicate that the C-terminal region, which is intact in ERK1b but missing from ERK1c, plays a role in the activation of ERKs by MEKs. Alternatively, it is possible that the conformation of CRS in ERK1b still allows recognition (but not strong interaction) of MEK1, while a bigger conformational change in ERK1c does not allow both activities.

Ubiquitination and phosphorylation are two of the most ubiquitous signals that regulate the fate of cells and tissues. However, while phosphorylation is a signal with a wide array of outcomes, such as activation, inhibition, binding, or dissociation, ubiquitination is more restricted in function, as polyubiquitination seems to be a signal for destruction (13, 20), and monoubiquitination often serves as a cellular targeting device (16, 36). Polyubiquitination seems to play a role in the regulation of ERKs in late stages after stress signals (22), while monoubiquitination was not reported to occur in ERKs, indicating that both these processes are not common regulatory mechanisms for ERKs. Interestingly, by blocking the proteosome system, we also found that unlike ERK1, ERK1c can be monoubiquitinated but not polyubiquitinated upon the addition of the proteosome inhibitor MG132. However, monoubiquitination is not a signal for proteosomal degradation (13), and there was no significant change in the amount of the ERK1c protein upon addition of the inhibitor. Therefore, it is unlikely that ERK1c is directly regulated by degradation in the proteosome, although inhibition of the proteosome seems to indi-

rectly stabilize the monoubiquitinated ERK1c. The nature of this indirect link between the appearance of monoubiquitinated ERK1c and proteosomal degradation is not clear. One possibility is that ERK1c molecules undergo a small amount of constant monoubiquitination, which directs them to the Golgi apparatus, especially in confluent cell cultures (Fig. 8). From these compartments, ERK1c may undergo polyubiquitination that was not detected in our experimental setup, probably due to lack of extraction. However, a more likely explanation is that monoubiquitination is not a direct effect of proteosome inhibition. Indeed, we observed the appearance of a monoubiquitinated ERK1c (50 kDa, Fig. 7) (and occasionally diubiquitinated ERK1c also) under conditions of high cell density and prolonged serum starvation (2 days [not shown]). Since under similar conditions we also observed enhanced Golgi staining (Fig. 8C), our results indicate that the monoubiquitination of ERK1c is not linked to its degradation and may occur under various conditions when a specific subcellular target of ERK1c (e.g., Golgi apparatus) is required.

Another question that arises from our results is the site of monoubiquitination on ERK1c. The consensus sequence for monoubiquitination has been identified as a stretch of leucine and acidic residues (26). Interestingly, a similar sequence is found in ERK1c at residues 265 to 304, although it contains a gap of unrelated sequence in residues 277 to 297. It should be noted that this sequence also appears in ERK1 and ERK2 proteins that are not monoubiquitinated under our conditions. It is possible that the conformational change induced in ERK1c exposes the site, which is blocked and cannot be monoubiquitinated in ERK1.

The role of the ERK cascade in Golgi fragmentation is not fully understood. The Golgi apparatus of mammalian cells is organized into stacks of cisternae, which are anchored in the pericentriolar region (37). Once the cell enters mitosis, the pericentriolar stacks of Golgi cisternae undergo extensive fragmentation, and the fragments are dispersed throughout the cytosol. This process was initially shown to be mediated by MEKs without a clear involvement of ERK1 or ERK2 (1). The Golgi protein GRASP55, which may be the protein that converts the Golgi stacks into small fragments, was shown to be phosphorylated in the beginning of mitosis in a MEK-dependent manner (19). This phosphorylation seems to enhance its fragmenting activity; therefore, it is possible that the ERK cascade regulates Golgi fragmentation via this GRASP55 phosphorylation (19). Moreover, using phosphorylation site-specific ERK antibodies, it was shown that ERK phosphorylated on the Tyr residue (pY-ERK) within the TEY activation sequence is found constitutively in the nucleus and accumulates in the Golgi complex of cells that are in late G_2 or early mitosis of the cell cycle (8). However, the exact nature of the ERKs that were identified by these antibodies is not clear. Moreover, at this time, we have not found a link between ERK1c and regulation of the cell cycle. On the other hand, we did notice that the Golgi apparatus undergoes fragmentation in overconfluent cell cultures, and we show that ERK1c plays an important role in this cell density-dependent event (Fig. 10), but the role of ERK1c is not yet known.

The expression of ERK1b or ERK1c in the organism may be important for the signaling specificity of ERKs, because the ERK cascade is a central signaling mechanism that plays a role in many distinct and even opposing cellular processes. Therefore, studying the mechanism that allows different specificities for ERKs under different conditions may contribute to understanding the function of this cascade. Previous reports suggested that the specificity of the cascade may be determined in part by the strength, duration, and compartmentalization of the transmitted signal (32). Here we show that the specificity of ERK signaling can also be determined by the multiple ERK isoforms with different modes of regulation. For example, the localization of ERK1c in the Golgi apparatus may suggest that it transmits the unique Ras signal in that location (10). Additional putative spliced forms of ERKs could participate in determining the specificity and thus contribute to the wide variety of functions of this cascade.

In summary, we report here on the identification of ERK1c, an alternatively spliced form of ERK1 with a predicted mass of 40 kDa, which migrates together with ERK2 on SDS-polyacrylamide gels (42 kDa). The relative amount of ERK1c expression is substantial, and its level of mRNA was estimated to reach ~10% of the ERK1 level. ERK1c has a slower kinetics of activation by MEKs than ERK1 does, and this slower activation together with its lack of sensitivity to phosphatases are probably the reason for its different kinetics of activation in response to various extracellular stimuli. Since this isoform is less sensitive to phosphatases, it demonstrates a relatively high basal activity, and it is possible that many previous reports on the basal activity of ERK2 were in fact due to the activity of ERK1c. We found that ERK1c can be monoubiquitinated in response to several conditions, which may be related to its Golgi localization, as both events are enhanced with increased cell density and MG132 treatment. Overexpression of ERK1c results in Golgi fragmentation, and dominant-negative ERK1c inhibits the cell density-induced Golgi fragmentation, indicating that ERK1c may mediate MEK-induced regulation of the Golgi apparatus in overconfluent cells. Overall, the differential regulation and localization of ERK1c suggest that it may extend the specificity of the ERK cascade upon stimulation by different extracellular stimuli.

ACKNOWLEDGMENTS

We thank Y. Yarden and S. Oved for the HA-ubiquitin construct.

This work was supported in part by grants from the Israel Academy of Sciences and Humanities and from the Women Health Center in the Weizmann Institute of Science (to R.S.) and the Swiss National Science Foundation and the Swiss Friends of the Weizmann Institute (to D.M.A.).

REFERENCES

1. **Acharya, U., A. Mallabiabarrena, J. K. Acharya, and V. Malhotra.** 1998. Signaling via mitogen-activated protein kinase kinase (MEK1) is required for Golgi fragmentation during mitosis. Cell **92:**183–192.
2. **Bott, C. M., S. G. Thorneycroft, and C. J. Marshall.** 1994. The sevenmaker gain-of-function mutation in p42 MAP kinase leads to enhanced signalling and reduced sensitivity to dual specificity phosphatase action. FEBS Lett. **352:**201–205.
3. **Boucher, M. J., D. Jean, A. Vezina, and N. Rivard.** 2004. Dual role of MEK/ERK signaling in senescence and transformation of intestinal epithelial cells. Am. J. Physiol. Gastrointest. Liver Physiol. **286:**G736-G746. (First published 30 December 2003; http://ajpgi.physiology.org/cgi/content/full/286/5/G736.)
4. **Boulton, T. G., and M. H. Cobb.** 1991. Identification of multiple extracellular signal-regulated kinases (ERKs) with antipeptide antibodies. Cell Regul. **2:**357–371.
5. **Boulton, T. G., S. H. Nye, D. J. Robbins, N. Y. Ip, E. Radziejewska, S. D. Morgenbesser, R. A. DePinho, N. Panayotatos, M. H. Cobb, and G. D. Yancopoulos.** 1991. ERKs: a family of protein-serine/threonine kinases that

are activated and tyrosine phosphorylated in response to insulin and NGF. Cell **65:**663–675.
6. **Boussif, O., F. Lezoualc'h, M. A. Zanta, M. D. Mergny, D. Scherman, B. Demeneix, and J. P. Behr.** 1995. A versatile vector for gene and oligonucleotide transfer into cells in culture and in vivo: polyethylenimine. Proc. Natl. Acad. Sci. USA **92:**7297–7301.
7. **Camarillo, I. G., B. E. Linebaugh, and J. A. Rillema.** 1997. Differential tyrosyl-phosphorylation of multiple mitogen-activated protein kinase isoforms in response to prolactin in Nb2 lymphoma cells. Proc. Soc. Exp. Biol. Med. **215:**198–202.
8. **Cha, H., and P. Shapiro.** 2001. Tyrosine-phosphorylated extracellular signal-regulated kinase associates with the Golgi complex during G_2/M phase of the cell cycle: evidence for regulation of Golgi structure. J. Cell Biol. **153:**1355–1367.
9. **Chang, L., and M. Karin.** 2001. Mammalian MAP kinase signalling cascades. Nature **410:**37–40.
10. **Chiu, V. K., T. Bivona, A. Hach, J. B. Sajous, J. Silletti, H. Wiener, R. L. Johnson II, A. D. Cox, and M. R. Philips.** 2002. Ras signalling on the endoplasmic reticulum and the Golgi. Nat. Cell Biol. **4:**343–350.
11. **English, J. M., C. A. Vanderbilt, S. Xu, S. Marcus, and M. H. Cobb.** 1995. Isolation of MEK5 and differential expression of alternatively spliced forms. J. Biol. Chem. **270:**28897–28902.
12. **Gille, H., A. D. Sharrocks, and P. E. Shaw.** 1992. Phosphorylation of transcription factor p62TCF by MAP kinase stimulates ternary complex formation at c-fos promoter. Nature **358:**414–417.
13. **Glickman, M. H., and A. Ciechanover.** 2002. The ubiquitin-proteasome proteolytic pathway: destruction for the sake of construction. Physiol. Rev. **82:**373–428.
14. **Gonzalez, F. A., D. L. Raden, M. R. Rigby, and R. J. Davis.** 1992. Heterogeneous expression of four MAP kinase isoforms in human tissues. FEBS Lett. **304:**170–178.
15. **Gupta, S., T. Barrett, A. J. Whitmarsh, J. Cavanagh, H. K. Sluss, B. Derijard, and R. J. Davis.** 1996. Selective interaction of JNK protein kinase isoforms with transcription factors. EMBO J. **15:**2760–2770.
16. **Haglund, K., P. P. Di Fiore, and I. Dikic.** 2003. Distinct monoubiquitin signals in receptor endocytosis. Trends Biochem. Sci. **28:**598–603.
17. **Han, J., J. D. Lee, Y. Jiang, Z. Li, L. Feng, and R. J. Ulevitch.** 1996. Characterization of the structure and function of a novel MAP kinase kinase (MKK6). J. Biol. Chem. **271:**2886–2891.
18. **Hendricks, L. C., C. A. Gabel, K. Suh, and M. G. Farquhar.** 1991. A 58-kDa resident protein of the cis Golgi cisterna is not terminally glycosylated. J. Biol. Chem. **266:**17559–17565.
19. **Jesch, S. A., T. S. Lewis, N. G. Ahn, and A. D. Linstedt.** 2001. Mitotic phosphorylation of Golgi reassembly stacking protein 55 by mitogen-activated protein kinase ERK2. Mol. Biol. Cell **12:**1811–1817.
20. **Karin, M., and Y. Ben-Neriah.** 2000. Phosphorylation meets ubiquitination: the control of NF-κB activity. Annu. Rev. Immunol. **18:**621–663.
21. **Langlois, W. J., T. Sasaoka, A. R. Saltiel, and J. M. Olefsky.** 1995. Negative feedback regulation and desensitization of insulin- and epidermal growth factor-stimulated p21ras activation. J. Biol. Chem. **270:**25320–25323.
22. **Lu, Z., S. Xu, C. Joazeiro, M. H. Cobb, and T. Hunter.** 2002. The PHD domain of MEKK1 acts as an E3 ubiquitin ligase and mediates ubiquitination and degradation of ERK1/2. Mol. Cell **9:**945–956.
23. **Marshall, C. J.** 1995. Specificity of receptor tyrosine kinase signaling: transient versus sustained extracellular signal-regulated kinase activation. Cell **80:**179–185.
24. **Pages, G., S. Guerin, D. Grall, F. Bonino, A. Smith, F. Anjuere, P. Auberger, and J. Pouyssegur.** 1999. Defective thymocyte maturation in p44 MAP kinase (Erk 1) knockout mice. Science **286:**1374–1377.
25. **Peng, X., J. M. Angelastro, and L. A. Greene.** 1996. Tyrosine phosphorylation of extracellular signal-regulated protein kinase 4 in response to growth factors. J. Neurochem. **66:**1191–1197.
26. **Polo, S., S. Sigismund, M. Faretta, M. Guidi, M. R. Capua, G. Bossi, H. Chen, P. De Camilli, and P. P. Di Fiore.** 2002. A single motif responsible for ubiquitin recognition and monoubiquitination in endocytic proteins. Nature **416:**451–455.
27. **Pulido, R., A. Zuniga, and A. Ullrich.** 1998. PTP-SL and STEP protein tyrosine phosphatases regulate the activation of the extracellular signal-regulated kinases ERK1 and ERK2 by association through a kinase interaction motif. EMBO J. **17:**7337–7350.
28. **Raman, M., and M. H. Cobb.** 2003. MAP kinase modules: many roads home. Curr. Biol. **13:**R886–R888.
29. **Reszka, A. A., R. Seger, C. D. Diltz, E. G. Krebs, and E. H. Fischer.** 1995. Association of mitogen-activated protein kinase with the microtubule cytoskeleton. Proc. Natl. Acad. Sci. USA **92:**8881–8885.
30. **Robinson, M. J., and M. H. Cobb.** 1997. Mitogen-activated protein kinase pathways. Curr. Opin. Cell Biol. **9:**180–186.
31. **Rubinfeld, H., T. Hanoch, and R. Seger.** 1999. Identification of a cytoplasmic-retention sequence in ERK2. J. Biol. Chem. **274:**30349–30352.
32. **Rubinfeld, H., and R. Seger.** 2004. The ERK cascade as a prototype of MAPK signaling pathways. Methods Mol. Biol. **250:**1–28.
33. **Schaeffer, H. J., A. D. Catling, S. T. Eblen, L. S. Collier, A. Krauss, and M. J. Weber.** 1998. MP1: a MEK binding partner that enhances enzymatic activation of the MAP kinase cascade. Science **281:**1668–1671.
34. **Seger, R., and E. G. Krebs.** 1995. The MAPK signaling cascade. FASEB J. **9:**726–735.
35. **Seger, R., D. Seger, F. J. Lozeman, N. G. Ahn, L. M. Graves, J. S. Campbell, L. Ericsson, M. Harrylock, A. M. Jensen, and E. G. Krebs.** 1992. Human T-cell Map kinase kinases are related to yeast signal transduction kinases. J. Biol. Chem. **267:**25628–25631.
36. **Shmueli, A., and M. Oren.** 2004. Regulation of p53 by Mdm2: fate is in the numbers. Mol. Cell **13:**4–5.
37. **Sutterlin, C., P. Hsu, A. Mallabiabarrena, and V. Malhotra.** 2002. Fragmentation and dispersal of the pericentriolar Golgi complex is required for entry into mitosis in mammalian cells. Cell **109:**359–369.
38. **Tanoue, T., M. Adachi, T. Moriguchi, and E. Nishida.** 2000. A conserved docking motif in MAP kinases common to substrates, activators and regulators. Nat. Cell Biol. **2:**110–116.
39. **Tanoue, T., and E. Nishida.** 2002. Docking interactions in the mitogen-activated protein kinase cascades. Pharmacol. Ther. **93:**193–202.
40. **Tanoue, T., and E. Nishida.** 2003. Molecular recognitions in the MAP kinase cascades. Cell Signal. **15:**455–462.
41. **Tournier, C., A. J. Whitmarsh, J. Cavanagh, T. Barrett, and R. J. Davis.** 1999. The MKK7 gene encodes a group of c-Jun NH_2-terminal kinase kinases. Mol. Cell. Biol. **19:**1569–1581.
42. **Wolf, I., H. Rubinfeld, S. Yoon, G. Marmor, T. Hanoch, and R. Seger.** 2001. Involvement of the activation loop of ERK in the detachment from cytosolic anchoring. J. Biol. Chem. **276:**24490–24497.
43. **Xu, R., R. Seger, and I. Pecht.** 1999. Cutting edge: extracellular signal-regulated kinase activates syk: a new potential feedback regulation of Fc epsilon receptor signaling. J. Immunol. **163:**1110–1114.
44. **Yan, C., H. Luo, J. D. Lee, J. Abe, and B. C. Berk.** 2001. Molecular cloning of mouse ERK5/BMK1 splice variants and characterization of ERK5 functional domains. J. Biol. Chem. **276:**10870–10878.
45. **Yao, Y., W. Li, J. Wu, U. A. Germann, M. S. Su, K. Kuida, and D. M. Boucher.** 2003. Extracellular signal-regulated kinase 2 is necessary for mesoderm differentiation. Proc. Natl. Acad. Sci. USA **100:**12759–12764.
46. **Yung, Y., Y. Dolginov, Z. Yao, H. Rubinfeld, D. Michael, T. Hanoch, E. Roubini, Z. Lando, D. Zharhary, and R. Seger.** 1997. Detection of ERK activation by a novel monoclonal antibody. FEBS Lett. **408:**292–296.
47. **Yung, Y., Z. Yao, D. M. Aebersold, T. Hanoch, and R. Seger.** 2001. Altered regulation of ERK1b by MEK1 and PTP-SL, and modified Elk1-phosphorylation by ERK1b are caused by abrogation of the regulatory C-terminal sequence of ERKs. J. Biol. Chem. **276:**35280–35289.
48. **Yung, Y., Z. Yao, T. Hanoch, and R. Seger.** 2000. ERK1b, a 46-kDa ERK isoform that is differentially regulated by MEK. J. Biol. Chem. **275:**15799–15808.
49. **Zheng, C. F., and K. L. Guan.** 1993. Properties of MEKs, the kinases that phosphorylate and activate the extracellular signal-regulated kinases. J. Biol. Chem. **268:**23933–23939.